NASA Contractor Report 179634

Stability and Rheology of Dispersions of Silicon Nitride and Silicon Carbide

Donald L. Feke
Case Western Reserve University
Cleveland, Ohio

June 1987

Prepared for
Lewis Research Center
Under Grant NAG3-468

National Aeronautics and
Space Administration

Contents

Summary

The structure and properties of structural ceramic components depend directly on the density, homogeneity, and micromechanical properties of their green compacts. Improved processing and casting techniquies for the formation of green bodies thus have the potential to increase the reliability, fracture strength, and toughness, as well as the cost effectiveness of structural ceramics.

In the wet processing of ceramics, dispersion characteristics (such as the degree of agglomeration and rheology of the slip) and the interfacial chemistry between the solids and suspending fluids are necessarily linked to each other. Similarly, the interfacial chemistry of the powder in suspension is rooted to the powder synthesis conditions. The following diagram illustrates this spectrum of connections:

Component Properties $\Longleftrightarrow$ Structure of Casting $\Longleftrightarrow$ Colloidal Characteristics $\Longleftrightarrow$ Interfacial Chemistry $\Longleftrightarrow$ Powder Synthesis

The relationship between structural properties of the cast body and colloidal parameters has been established by a number of investigators[1-4]. It is known that measurement of colloidal parameters like surface charge and zeta potential is important in predicting dispersion quality and rheology in ceramic slips. However, control and manipulation of the colloidal parameters to give optimum dispersion qualities is desirable from a practical viewpoint. Additionally, the two rightmost links in the spectrum above, that is, the connection between the interfacial chemistry and the dispersion characteristics, and the relation

between the interfacial chemistry and the powder synthesis route, have not been sufficiently studied for most ceramic systems of interest.

It was the primary goal of this research to investigate thoroughly the connections between the various chemical factors described above that influence the structural properties of ceramic components. Because of their high strength-to-weight ratio, low thermal expansion coefficient, and inertness to many common corrosives, our studies have focussed on non-oxide ceramics, particularly silicon carbide and silicon nitride.

Often, attempts to predict or control processing behavior are frustrated by the variability, either batch-to-batch or manufacturer-to-manufacturer, of the dispersion properties exhibited by seemingly identical powders. In part, the lack of dispersion characterization and modification strategies explicitly developed for ceramic slips has compounded these difficulties. Attempts to borrow concepts, theories, and experimental techniques from traditional colloid science and apply them to ceramic dispersions have met with varying degrees of success. Because of the high degree of coupling between solution and interfacial chemistry in ceramic dispersions, and because practical ceramic slips have high solids content, neither of which are significant factors in traditional colloidal systems, new techniques and models need be developed.

Our thesis was that the source of the processing variability could be determined from identifying the true interfacial chemistry of the powders and eliminated by modifying the powders so that the native chemistry becomes active in the ceramic slips. In order to do this, we developed a surface titration methodology that distinguishes between solution and interfacial chemistry; thus we were enabled to reliably measure double-layer characteristics. Based on

these studies, we established pretreatment strategies to reduce the effects of powder surface contaminants that manifest themselves as artifacts in the dispersion behavior.

Additionally, we investigated powder modification strategies for the ultimate goal of achieving an active control over the dispersion behavior, and hence, the casting process. These modification strategies were applied to the ceramic powders as they were dispersed in slips. To complement this effort, a predictive model accurately relating the interfacial and solution chemistries of ceramic dispersions was formulated. No previous models reported in the literature are adequately successful at simultaneously relating both surface charge and zeta potential to solution chemistry. The hybrid-site model we have developed can be successfully applied to ceramic dispersions for this purpose.

Two other aspects of this research were coincident with the studies described above. In one, the effectiveness of pretreatment and modification strategies applied to the powders in the colloidal state on permanently altering the interfacial chemistry of the powders was studied by a variety of surface spectroscopic techniques. Preliminary results show that the interfacial characteristics of the powders do indeed retain some memory of the colloidal treatment, and that modifications to the powders in the dispersed state have a lasting effect on the interface in the dried state. In the second, the effectiveness of employing the powder pretreatment and modification strategies in improving the rheology and the microstructure formed during compaction of the ceramic slips is being investigated. At this stage, the results are inconclusive and incomplete.

1. Introduction

Techniques currently under investigation for forming silicon nitride and silicon carbide components from powders include slip casting, hot pressing, injection molding, and sol gel routes. Each of these methods produces a green body which is then sintered. An alternate method for forming both silicon nitride and silicon carbide products is reaction bonding from a silicon green body precursor. In all of these methods, inhomogeneities present in the original green body remain in the final sintered product and thus affect the final mechanical properties. Efforts to sinter silicon nitride and silicon carbide ceramics without addition of or with reduced amounts of sintering aids have led to investigation of sub-micron size ceramic powders. In this instance, both particle size and packing homogeneity strongly affect the final compact quality.

The research described herein focuses on improving the green structure by obtaining better dispersion and stability of the ceramic powders in simple powder-solvent colloidal systems. This work attempts to provide the first thorough assessment of the surface chemistry responsible for the colloidal behavior of these ceramic dispersions as well as the development of characterization techniques appropriate for these systems. The particular systems studied were composed of commercially available high-purity, fine silicon nitride and silicon carbide powders dispersed in aqueous media. These model systems contained only powder, water, supporting electrolyte (salt) and acid/base -- no surfactants, viscosity modifiers, etc. were present.

Much of the literature[5-6] suggests that the surface of any silicon

substrate exposed to the ambient environment will contain at least a monolayer of silica. Silicon nitride and silicon carbide oxidize by mechanisms similar to silicon. Recently, Rahaman[7] reported preliminary results revealing a native 3-5 nm amorphous oxide or silicon oxynitride layer on the surface of several commercial silicon nitride powders. Likewise, he found a 3-5 nm silica layer on silicon carbide. Busca, et.al.[8] published an extensive study of the surface properties of a high surface area silicon nitride which was prepared by nitridation of amorphous silica with ammonia at 1300°C. The presence of SiOH (surface silanols), Si-NH-Si (imido groups), and SiH (silane) was observed as well as was evidence of basic nitrogens bonded to three silicon atoms. They cite an increased basicity of silicon nitride with respect to that observed for silica: this is attributed to the presence of the imido and basic nitrogen groups. In addition, they also report a slight reduction in the acid strength of the silanol groups on silicon nitride, as compared to silanols found on silica surfaces. The reduction in the silanol acidity is attributed to the smaller effect of nitrogen in silicon nitride bonds compared to oxygen in silica bonds.

Busca dids not observe any $Si-NH_2$ (amido) groups on the surface after vacuum pretreatment of the powders at temperatures up to 400°C. Further evacuation and heating to 200 - 300°C condenses the near-lying hydrogen bonded silanols. After the initial activation of the amorphous silicon nitride (by evacuation at 400°C), Busca also notes that hydrogen-bonded ammonia is completely desorbed by evacuation at room temperature.

Our investigations[9] of the surface of commercial high surface area silicon nitride and silicon carbide using DRIFT have shown both the existence of an SiO_x

surface layer and some amine/ammonia species on as-received and heat treated silicon nitride powders. Spectra for raw silicon nitride powders contain a sharp peak at 3750 cm^{-1}, indicating the presence of free silanols, as well as a broad band at 3000-3500 cm^{-1}, which suggests the presence of adsorbed molecular water (3400 cm^{-1}), hydrogen bonded silanols (3650 and 3550 cm^{-1}), and an amine species (3320 cm^{-1}). The broad band was greatly reduced, but not eliminated by heat treatment in argon at 500°C for 24 hours. The amine (N-H) stretch was attributed to some combination of the following three surface species: an ammonia molecule hydrogen bonded to a silanol (I), a primary silicon amine (II), or a secondary surface amine (III).

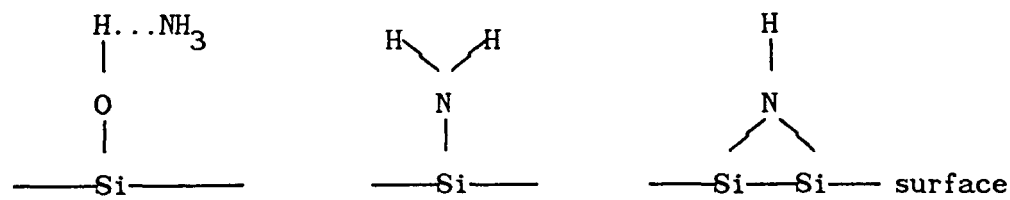

I)Ammonia H-bonded to silanol

II)Primary surface amine

III)Secondary surface amine

Much is known of the surface chemistry of silica[10]. The surface species native to silica are generally classified as 1) free silanols, 2) hydrogen-bonded (adjacent silanols) or 3) siloxanes:

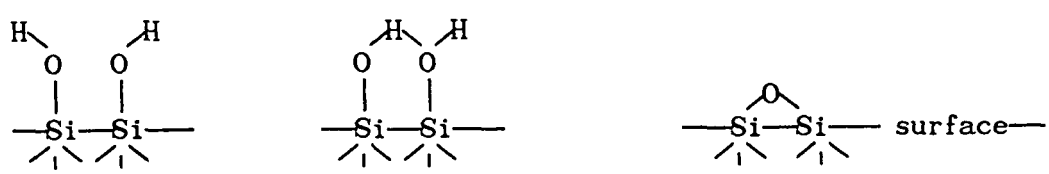

1)free surface silanol

2)hydrogen-bonded surface silanol

3)siloxane

The silanol groups are hydrophilic while the siloxanes are hydrophobic. A fully hydrated silica surface (containing no siloxanes) is expected to have approximately 4.6 Si-OH surface sites/nm^2. For fully hydrated amorphous silica, Armistead[11] observes 4.5 surface silanols/nm^2. Using probe molecules such as ammonia, he determined that the silanol population was split such that 3.2 sites/nm^2 are hydrogen bonded and the remaining 1.3 are free silanols. Yates[12] determined the number of rapidly exchangable protons for a fully hydrated, non-porous silica by aqueous titration in strong electrolyte and estimated a limiting silanol site density of 3.5 ionizable sites/nm^2. Hence it is probable that some of the surface silanols on commercial silica do not deprotonate in readily achievable aqueous environments.

On the other hand, a fully dehydrated silica surface would consist entirely of siloxanes, which would neither protonate nor deprotonate in the presence of acid or base. Baking in an inert environment at 1000^{o}C for 24 hours will reportedly completely dehydrate a silica surface[10]. Most manufacturing processes for silicon nitride and silicon carbide subject the powders to inert or reducing environments at temperatures well exceeding 1000^{o}C during crystallization. Hydration of the powders probably occurs during storage.

In addition to the many studies investigating the adsorption/desorption of water on silica surfaces, there have also been numerous studies of the adsorption/desorption of ammonia and amine vapors on various silica surfaces. Ammonia is adsorbed stoichiometrically on free (non-hydrogen bonded) silanol groups[13], as are most of the amines[14]. Boyle and Gaw[15] report that both physisorption and chemisorption of ammonia are important, presumably due to the

strong hydrogen bonding which can exist between the silanol groups and the adsorbant. Bliznakov and Polikarova[16] report irreversibly bound ammonia below 70°C. Shifts in the infrared adsorption band of the OH stretch have been observed and are generally acknowledged to confirm the hydrogen bonding of ammonia and the weakly basic amines to the surface silanols on silica.

1.1 Research Objectives

The experimental objectives of this research were four-fold: 1) to characterize the colloid behavior of commercially available silicon carbide and silicon nitride powders, 2) to develop modification and processing strategies which should provide improved green ceramic uniformity, 3) to investigate the permance of the modification strategies on the interfacial chemistry of silicon nitride powders as well as sillicon carbide powders and fibers, and 4) to examine the benefits of the colloidal processing strategies on slip rheology and compaction behavior.

Prediction of the stability and rheology of ceramic dispersions is important for a variety of fundamental and pragmatic reasons, and many models have been proposed to relate double-layer phenomena to the interfacial characteristics and solution chemistry of suspensions. Early models to predict the behavior of hydrous oxides defined hydrogen and hydroxyl ions as the potential determining ions, which implies that solution pH determines surface charge and potential. Later work recognized that adsorption of supporting electrolyte ions to surface sites also affects the double-layer behavior. These models have been successfully applied to several oxide systems such as titania, alumina, and iron, but somewhat less successfully applied to silica. Good

reviews have been published by Healy and White[17], Wiese et al.[18] and James and Parks[19].

In all of these models, the interface is assumed to be populated by only one type of active site. In actuality, surface sites of a given chemistry may show different degrees of double-layer activity due to steric effects; isolated hydroxyls being different than vicinal hydroxyls, for example. In addition, many materials may have more than one type of ionizable surface site. In this work, we have also developed a model for a hybrid-site interface containing a single amphoteric site as well as a monoprotic basic site such is characteristic of materials such as silicon nitride dispersions. Experimental results were interpreted in terms of this model.

2. Experimental Procedures

2.1 Selection and Preparation of Powders and Whiskers

Primary work has centered on two ultra-fine ceramic powders -- UBE SN-E10 α-silicon nitride (13 m^2/g), and Lonza UF-15 α-silicon carbide (15 m^2/g). Key experiments have been duplicated with three other silicon nitride powders manufactured by Denka (7 m^2/g), Toshiba (11 m^2/g) and Toya Soda (11 m^2/g). Silicon carbide whiskers manufactured by Arco were also studied. All of these materials are believed to be free of intentionally added manufacturing aids which could alter their colloidal behavior in a manner uncharacteristic of the species. However, the presence of surface contamination of the powders became apparent, and thus an unpredictable, history-dependent aspect to their interfacial chemistry was observed.

To resolve this problem, samples of the as-received materials were subjected to various pretreatment strategies in order to identify true differences in the native interfacial chemistry of the various powders and to differentiate artifacts due to the storage, handling, or manufacturing of these powders. Pretreatments included: 1)baking the powders at 500°C in Ar; 2)baking the powders at 300°C in oxygen; 3)washing the powders or whiskers in acidified electrolyte solutions; 4)washing the powders in pure deionized water; 5)drying water-washed powders at either 80°C in air, 500°C in Ar, or 300°C in oxygen; and 6)exposing the as-received dry powders to moderate vacuum (20 to 30 microns Hg absolute) followed by either no further treatment or washing in acidified electrolyte solution. Washing procedures included ultrasonic-aided dispersion of the dry powder followed by repeated cycles of centrifugation (1500xg for

30-60 min) and redispersion of the wet cake in the desired wash solution, either pure deionized water, or acidified electrolyte. Powders were baked for 20 hours in a 1-in pyrex-tube furnace; the argon used was 99.999% pure while the oxygen was house oxygen of indeterminate purity. Deionized water used to wash the powders or to prepare the electrolyte solutions was >17 megohm resistivity from a Nanopure water system (Barnstead/Sybron Corporation, Boston, MA). To ensure that there were no nonionic species affecting the titration measurements, several preliminary runs were repeated using triple distilled or deionized-then-distilled water. No difference was detected between the three water sources.

Literature supplied by the powder manufacturers was the primary source of information characterizing chemical purity, surface area, and particle size and morphology. Particle size distributions after various dispersion treatments were determined in our laboratory using a Sedigraph (Micromeretics, Princeton, NJ).

2.2 Titration of Surface Groups

Measurement of surface charge is a strong predictive parameter of dispersion behavior. Assuming that protons and hydroxyl groups are potential determining ions for silicon carbide and silicon nitride, then determination of surface charge can be accomplished using standard titration techniques pioneered by Overbeek[20] and Parks and de Bruyn[21]. In this methodology, the uptake of acid or base by a suspension is measured and compared to the uptake of acid or base by a reference solution of equivalent liquid volume. The difference between uptakes of the suspension and reference solution at corresponding pH values is

attributable to the participation of the solid surface in the titration. By normalizing with respect to the total surface area of solid present in the suspension, this difference can be interpreted as the proton adsorption density on the solid. The pH at which the uptake curves for the suspension and the reference solution intersect is the point of zero relative adsorption (PZRA).

Ionic strengths of the suspension are controlled through the addition of a comparatively large amount of background salt. Normally, the reference fluid is a pure electrolyte solution having the same ionic concentration as the suspension. However, in order to check for dissolution of the solid or desorption of any surface species into the suspending liquid, we also used centrates derived from mother suspensions as reference solutions. Participation of the background electrolyte was checked by comparing the results of the titrations of suspensions prepared at several different ionic concentrations. If all of the titration results intersect at a single pH value, it is probable that the electrolytes are indifferent (i.e. do not participate in the interfacial chemistry of the solid) and, consequently, the pH at the intersection is the point of zero charge (PZC).

The potentiometric titration system consisted of a Mettler DL40 Memotitrator (Mettler Instrument Corporation, Hightstown, NJ) capable of dispensing titrant increments as small as 0.001 ml at intervals of up to 2.5 hours apart, Schott Ag/AgCl reference and type H (low alkali error) glass pH electrodes, a glass sleeve junction salt bridge, a platinum grounding wire (in the titration cell solution), and an enclosed titration vessel blanketed by a wet argon purge.

In a titration experiment, fixed volumes of titrant are delivered to

suspensions judged to be at equilibrium according to some preset criteria. Typically, the equilibrium criterion chosen was for the suspension to exhibit less than a 0.04 unit change in the pH over a 5 sec interval; this resulted in titration times of 0.75 to 1 hour per sample. The effect of titration speed on the reported adsorption of proton or hydroxyl was observed by applying other equilibrium criteria (e.g. less than 0.02 pH unit change over 15 sec). In general, no significant differences were noted between the titration results obtained using the various equilibrium criteria.

Samples (2.5 to 25 % by weight solids) were prepared for titration by dispersing the dry powder in the acidified electrolyte solution using an ultrasonic probe. At these loadings, the dispersion contains enough powder to provide at least 25 m^2 of surface area in 40 ml of suspension. Centrates used as reference solutions were obtained by centrifuging an identically prepared suspension (1500 × g for 45 min). Unless otherwise noted in the results to follow, pure electrolyte solution was used as the reference for determining acid/base adsorption by the solid.

After completion of the preliminary experiments to determine appropriate pretreatment to eliminate the effects of storage and handling, a standardized titration method was adopted. All powders were exposed to vacuum for 24 hours prior to storage in a dry (less than 30 ppm water) argon environment. Immediately prior to titration, the dry powder was dispersed and washed 3 times in pH 3, 0.1 M KNO3 electrolyte solution followed by washing in pH 3, 0.001 M electrolyte solution. The sol was then allowed to equilibrate at room temperature for 2 - 3 hours before beginning the titration sequence.

In order to determine the point of zero charge (pzc) for a given material,

and hence to allow conversion of the adsorption isotherms from relative to absolute surface charge, it was necessary to titrate each sample at several ionic strengths. Since the chosen supporting electrolyte was indifferent (or at least the cation and anion exhibited the same adsorption energy) the curves crossed each other at a common intersection point (cip). Since we assume the surface charge to be solely due to protonation/deprotonation of surface sites, the cip must be the point of zero charge. Thus we could calculate the absolute surface charge by defining the charge at the cip to be identically equal to zero. In practice, this required titrating each sol four times in successively higher ionic strength solutions. After washing, the 0.001 M suspension was first titrated with 1.5 ml of 0.1 M KOH solution to an endpoint pH of 10.5-11.5. This basic suspension was then doped to 0.01 M KNO_3 by addition of neutral 1 M KNO3 solution and backtitrated to pH3 by addition of 0.1 M HNO_3 titrant. Dry KNO_3 salt was then added to increase the background electrolyte to 0.1 M KNO_3 and the suspension was again titrated with 1.5 ml of 0.1 M KOH. Finally, dry KNO3 was added to increase the background electrolyte to 1.0 M and then the basic suspension was titrated with 0.1M nitric acid. The pure 0.001 M electrolyte solution was titrated by an identical methodology for computation of the desired adsorption isotherms.

2.3 Milled Samples

While most titrations were performed using as-received powders, it was desirable to investigate the effects of milling on the surface species for the two primary materials, UBE silicon nitride and Lonza silicon carbide. To prevent contamination of the powders, the UBE powders were milled in a reaction

bonded silicon nitride mill with silicon nitride media and the Lonza UF-10 powder was milled in a silicon carbide mill with silicon carbide media. The silicon nitride powder was milled for 24 hours at 10 vol% in aqueous pH 3, 0.1M KNO_3. The 10 vol% silicon carbide was milled for 24 hours in pH 9, 0.1F aqueous ammonia solution. Particle size analysis before and after milling showed that milling eliminated the large (greater than 10 μm) agglomerates from the sols, but there was no apparent increase in surface area for either material after milling.

2.4 Observation of the Electrical Double Layer by ESA

ESA experiments were performed for 1 wt% sols of UBE and Toshiba silicon nitride powders in either 0.001F KNO_3 or NH_4Cl aqueous solution using the MBS System 8000 (Matec Instruments, Inc., Warwick, RI.) ESA unit. The powders were dispersed with an ultrasonic probe and then either nitric acid or potassium hydroxide (base) was added to achieve the desired pH. The experiments began at the equilibrium pH of the salt and powder, pH 5-7, and ESA measurements were obtained at selected pH values from pH 1.5 to 12.5. Separate samples were tested in the acid and base regions to minimize amplitude variation due to changing solids and salt concentrations as titrant was added. Some hysteresis was observed upon back titrating a sample which had been taken to high or low pH. The UBE samples and the Toshiba samples were tested on two different days Hence, due to calibration differences during setup one cannot quantitatively compare the magnitude of the ESA amplitudes recorded for the UBE samples to those recorded for the Toshiba samples. However, the the location of the pH at which the amplitude crosses zero (the pzc), should be unaffected by these

calibration differences.

2.5 Surface Spectroscopies

Various surface spectroscopic instruments available at CWRU were also used in this study. Auger Electron Spectroscopy (AES) was performed with a homebuilt instrument in the Department of Physics under the direction of Professor Richard Hoffman. Electron Spectroscopy for Chemical Analysis (ESCA or XPS) and Secondary Ion Mass Spectroscopy (SIMS) instruments were available in the Major Analytical Instruments Facility within the Department of Chemistry. Diffuse Reflectance Infrared Spectroscopy (DRIFT) equipment was available within the Department of Macromolecular Science.

3. Experimental Results and Discussion

3.1 Silicon Nitride

The effectiveness of the various pretreatment stategies on the titration results for silicon nitride powders is summarized in Figure 1. Here, the adsorption of a hydroxyl ion (or deprotonation of a silanol to produce a negatively charged site) is denoted as a adsorption of a "negative" proton. The titration curve for as-received powder, curve (e), indicates a high point of zero realative adsorption (PZRA) -- pH 9 -- and the existence of amphoteric surface sites. Curves (c) and (d) were obtained for powder that was exposed to vacuum but to no further treatment. The replicate curves demonstrate the reproducibility of the titration results when sample history is carefully manipulated. Note that the effect of the vacuum treatment is to shift the apparent PZRA to lower pH. These results indicate that some basic species, present on the as-received powders, are removed by this pretreatment. Curve (a) contains the titration results for a vacuum-treated and acid-washed silicon nitride powder. This treatment results in a powder that exhibits a low PZRA (pH 3) and clearly lacks the relatively basic species observed with the as-received powders.

Interpretation of the disparate results shown in Figure 1 can be reconciled by considering the participation of the liquid phase in the titration methodology. If the powder contains some surface species that desorbs upon suspension of the powder, then titration of the suspension will simultaneously record the participation of the solid surface, the background electrolyte solution, and the desorbed species. To test this hypothesis, centrate derived

from the same powder which led to the results of Figure 1, curve (c) was titrated. When this liquid (which apparently contains desorbed species) was used as the reference for the calculation of the titration response of the solid, the results originally calculated using the pure electrolyte as reference and reported as curve (c) are corrected to give curve (b) in Figure 1. Note that these results, which are analytically compensated for the presence of desorbed species in the suspending liquid, closely follow the results obtained directly for the vacuum-treated and acid-washed powder, curve (a). Thus, this particular combination of pretreatments apparently yields a well-cleaned powder. Accurate interpretation of the titration methodology thus depends upon isolating surface chemistry from solution chemistry, or upon correcting for the presence of desorbed species in the liquid phase.

Among the pretreatment techniques employed to remove the adsorbed surface species, we also considered baking in inert or oxidizing atmospheres. Baking the powders in pure oxygen at 300^{o}C or in argon at 500^{o}C for 18 to 24 hours yielded results similar to those depicted in Figure 1, curves (c) and (d); apparently, these pretreatments are capable of removing physisorbed species but do not change the extent of oxidation or hydration of the native powders. The most reliable method for removing the chemisorbed species was repeated dilution of the sol in acidified aqueous electrolyte. The effectiveness of the acid washing pretreatments varied with the pH and ionic strength of the wash fluid. Typically three or four washes were necessary to clean powders when the electrolyte concentration was 0.1M, while up to ten washes were needed when 0.001M electrolyte was used. Powders were assumed to be clean when the centrate from a wash cycle showed no titration activity relative to a pure electrolyte solution.

Additionally, we have found that well-cleaned silicon nitride powders will react with neutral or basic aqueous solution over a period of a few hours to reform the adsorbate. Our working hypotheses are that the predominate titratable surface species on silicon nitride is silanol and that the primary adsorbed species on as-received powders is ammonia, most of which is physisorbed, but some of which is apparently chemisorbed. This dual behavior is similar to the reported behavior of ammonia on silica[15].

Some precautions must be taken, however, to avoid artifacts due to surface silica dissolution in interpreting titration results. In order to gauge the amount of dissolution, titrations were performed wherein samples were first acidified to pH 3, titrated to pH 10, and then backtitrated to pH 3. Minimal hysteresis was observed in the titration of well-washed samples provided that the time lapse between completion of the acid-to-base titration and the beginning of the base-to-acid titration is less than 15 minutes. In addition, a minimum solids concentration providing at least 20 m^2 per sample is necessary for titration accuracy. We have varied the solids concentration from this minimum level up to 125 m^2 per sample (25 wt%) and have seen no effect on the calculated adsorption site density. These results indicate that dissolution of the powders contributes negligibly to the reported results.

Figure 2 compares the relative proton adsorption at 0.1 M KNO_3 for silicon nitride powders manufactured by four different commercial processes. Note the similarity between the titration fingerprints of these four materials. Figure 3 compares the results of Toya Soda silicon nitride titration directly with those of UBE powder at equivalent concentrations of indifferent electrolyte. Both of

these manufacturers use a silicon diimide decomposition process for manufacturing their powders. Different manufacturing lots of UBE powders (Figure 4) demonstrate similar reproducibility.

Despite the similarity in the relative adsorption isotherms, the cip's (and hence absolute surface charge) for the four materials shown in Figure 2 exhibit more variability. Toshiba powders exhibit a cip at very low pH (pH 3-4) and have such a low slope at the pzc that determination of the actual cip is difficult and error prone. UBE and GTE powders demonstrate a pzc close to neutral pH (pH 5.5-7). The Denka 9FW powder exhibits a very high pzc (pH 8.8). Although the four processes used to manufacture the UBE, Toshiba, GTE, and Denka silicon nitride powders are widely disparate, and the pzc for the various powders ranges from pH 4 to pH 9, only the Denka relative adsorption curves reveal a significantly different titration fingerprint. The Denka powder is also the only material which is milled to achieve particle size, so it is possible that its surface chemistry is influenced by an undetected milling aid, rather than by some variant native silicon nitride surface species.

Moreover, the cip for UBE powders was found to be dependent upon pretreatment conditions. Figure 5 shows the relative adsorption curves for the standard acid-wash pretreatment of UBE powder. Figure 6, contains the relative adsorption curves for UBE powder which was exposed to vacuum, but not acid washed. Comparison of these two figures reveals both a shift in the cip from pH 6 to 7 as well as an increase in slope of the curves around the pzc which produces a much more distinct cip for the unwashed material. In addition, the surface chemistry of UBE powders is sensitive to milling of the powder before titration. The powders titrated in Figures 7-9 were milled in a silicon nitride

mill with silicon nitride media as described in the experimental section. As with the unwashed powder in Figure 6, the cip is higher (pH 6.5 - 7) and the slope at the pzc is greater for these milled samples than for the well-washed material in Figure 5. In addition, the cip for well-washed, milled powders (Figures 7 and 8) is lower than that for the partially washed material shown in Figure 9. Hence, the chemisorbed species present on both the unwashed raw and milled powders affects both the cip and apparent surface charge gradient at the pzc. In addition, the surface species formed on the fresh silicon nitride surfaces exposed during milling are evidently either qualitatively or quantitatively different from those present on as-received powders.

3.2 Silicon Carbide

The standard pretreatment for silicon carbide powders which we have adopted is washing the powder in acidified electrolyte solution. The pretreatment of silicon carbide did not appear to be particularly critical to titration results. Some pretreatment to remove physisorbed species due to exposure to atmospheric contaminants during handling and storage appears necessary.

The pzc for the Lonza UF-15 silicon carbide (Figure 10) is apparently below pH 3 (no cip is discernable), hence no absolute surface charge calculations can be ascertained without additional information from other analytical techniques.concentration providing at least 20 m^2 per sample is necessary for titration accuracy. We have varied the solids concentration from this minimum level up to 125 m^2 per sample (25 wt%), and have seen no effect on the calculated adsorption site density. These results indicate that dissolution of the powders contributes negligibly to the reported results.

Typical titration results for well-washed UBE silicon nitride and Lonza UF-15 silicon carbide, shown in Figure 11 reveal a remarkable similarity between their titration behavior. These relative adsorption curves also resemble titration curves obtained in our laboratory for Cabosil silica This evidence suggests that after applying the pretreatments to the powders, the predominant titratable surface group on either silicon nitride or silicon carbide is silanol.

In summary, surface titration data suggest a pzc of less than pH 3 for both silicon carbide and silica powders, and show little difference in relative proton adsorption between manufacturers of silicon nitride or between the silanol site density of silicon carbide and silicon nitride. The titration curves are reminiscent of those reported for silica. The shifting of the silicon nitride pzc to higher pH (pH 4 to 7) indicates the presence of basic sites in addition to the acidic silanol sites; the variability in either site density or adsorption free energy of these basic sites is reflected in the range of pzc's reported for the various silicon nitride powders. Finally, with careful pretreatment, the surface titration data are both reproducible and representative of the native surface of the powders.

3.3 Relevance of Titration Results to Other Observations

Titration data suggest that silicon carbide and Toshiba silicon nitride should behave very similarly since the powders have approximately the same particle size, specific gravity, and surface charge at any particular pH. Aqueous dispersions of these powders should flocculate rapidly at low pH (near the pzc) and become increasingly more stable as the pH is increased.

Observation of the sedimentation behavior of Toshiba silicon nitride and Lonza silicon carbide dispersions are generally in agreement with these expectations--the dispersions are colloidally unstable at pH less than 3 (flocculate and sediment rapidly) while and sols made from clean powders are stable for long periods of time in pure (pH 7) deionized water. Zeta potential curves in 0.01M KNO3 suggest an isoelectric point (iep) for silicon carbide of pH 2.5-3.0, which is also in agreement with the titration results, while others[22] observed an iep of about pH 3 for Toshiba powders.

In stark contrast, colloidal stability of UBE and GTE silicon nitride is apparently controlled by more than just the titrable silanol surface species which we observed. The reported isoelectric point for UBE silicon nitride is in the pH 6 to 7 range[23-24], and for GTE silicon nitride, the iep is reported to occur between pH 5 to 6.5[24-26]. Furthermore, dispersions of powders washed in deionized water display rapid flocculation in neutral deionized water; dispersions of powders at low pH (pH < 2) remain in suspension for many days. This is in good agreement with the apparent pzc (pH 5.5 - 7) measured by titration of the UBE and GTE powders.

3.4 The Role of Ammonia

The main constituents which are removed from the surface of silicon nitride when the powders are washed in acidified electrolyte (or water) are ammonia and silica. For a raw UBE silicon nitride sample, dispersed at the standard 4.5 wt% solids in pH 3, 0.1M KNO3 solution, we observed the desorption of 82 μmoles of ammonia. This is equivalent to surface coverage of 0.21 sites/nm^2. The dissolved silica, while detectable in the titration of the centrate, was

undetected in a standard colorimetric test for free silica (i.e. less than 2 ppm, which is equivalent to less than 0.002 wt% of the original silicon nitride). Both the silicon nitride and silicon carbide powders were chemically stable within the time frame of the titration.

Although the silicon nitride samples to be milled were adjusted initially to pH 3, by the end of the 24 hours of milling, the sol had reached pH 9.5 (which is the pH equivalent of a 0.1F NH_3 solution.) Since most ceramic processes will include a milling step to disperse the powders, most ceramic processing will occur in the presence of ammonia. Hence, it is desirable to understand the role of ammonia in silicon nitride colloidal dispersions.

Initially, it was hypothesized that hydrolysis of the ammonia desorbed from the silicon nitride powder might be contributing to, if not the sole cause of, the observed stability of some silicon nitride powders at low pH (where the surface silanols would be uncharged). If the positively charged ammonium ions were specifically adsorbed to the silica surface, they could yield the positive surface potential observed in electrophoresis experiments. To test this hypothesis, silica, well-washed silicon nitride, and silicon carbide were titrated in solutions of 5×10^{-3} M KNO_3 doped with concentrations of 3×10^{-5} to 0.03 F ammonium nitrate. If ammonium ions were indeed being specifically adsorbed, then even small concentrations of ammonium nitrate would be expected to affect the titration curves. As shown in Figure 12, the ammonium ions demonstrated no specific adsorption for silica, silicon nitride, or silicon carbide.

Further evidence that ammonium ions are not specifically adsorbed to silicon nitride was demonstrated by the results of ESA tests of UBE and Toshiba

powders in KNO_3 compared to NH_4Cl. Figure 13 demonstrates two important results: 1) the KNO_3 results are identical to those produced for the NH_4Cl electrolyte (within experimental error), and 2) the electrophoretic behavior of Toshiba silicon nitride very closely parallels that of silica[27] and silicon carbide, while the behavior of UBE silicon nitride is strikingly different from silica.

To further try to understand the difference between silicon nitride and silicon carbide surface chemistry, an attempt was made to alter the surface of Lonza UF-10 silicon carbide powder by milling powder for 24 hours in 0.1F, pH 9 ammonia solution. This experiment tested whether the presence of ammonia could affect the surface groups which are formed when fresh silica is produced by hydrolysis of the freshly exposed powder surfaces. Figure 14 shows that milling silicon carbide in the presence of ammonia had no effect on the relative adsorption isotherms. In contrast to the Lonza UF-15 material shown in Figure 10, the coarser, milled UF-10 silicon carbide shown in Figure 14 exhibits a cip at pH 3. This material bears a great resemblance to the Toshiba silicon nitride (Figure 15).

3.5 Permanence of the Colloidal Treatments

Although the pretreatment and modification strategies were demonstrated to influence dispersion characteristics, it was desirable to ascertain whether these procedures had any residual effect on the interfacial chemistry. In order to examine the capability of the ceramic materials to retain some memory of the colloidal treatments, a series of experiments were conducted in which the powders and whiskers were washed in solutions with pH less than, greater than,

or approximately equal their nominal PZC. The resulting solids were then centrifuged from suspension and dried under mild conditions. The residual interfacial chemistry was examined using the surface spectroscopies available. Depth profiling was accomplished in the Auger analysis by sputtering with an argon ion beam.

Figures 16, 17, and 18, which typify the preliminary trends, show the observed surface composition as a function of sputtering time. All of the materials showed some residual memory of the colloidal pretreatment. While the results presented for zero sputtering time are undoubtedly affected by contaminants or other precipitants deposited during the drying of the solids following the colloidal treatment, it is clear that the interface deeper than the outer surace has been shifted in chemical composition. This result points to the possibility of providing modified ceramic materials in the dry state, that will possess desirable colloidal characteristics when wet processed.

4. The Hybrid Site Model

We adopt the interface model of Davis, James, and Leckie[28]. Figure 19 defines the location of the various equipotential surfaces for the double layer. The absolute surface charge density σ_o and surface potential ψ_o are defined at the fixed plane at the actual surface. Some counterions, which specifically complex with the surface sites, are defined to lie in a second fixed plane with charge density σ_β and potential ψ_β. The extent of the complexation with the surface sites can be described by equilibrium constants, much as the extent of dissociation of an acid or base is described by its pK_a. The net charge density at either of the two inner planes can be found by summing the number density of the charged groups at that plane. The remaining counterions which would normally complete the Stern layer are contained between the β plane and the beginning of the diffuse layer. The diffuse part of the double layer begins at plane d and extends outward until the ion concentration and the electrical potential are equal to that in the bulk solution.

At any given position in the interface, the charge density and potential are related to the distribution of the various ionic species between the interface and the bulk fluid. Standard formulae are available to link these variables to each other.

If we assume that constant capacitances exist within the regions defined by the two fixed planes and the plane marking the beginning of the diffuse layer, the charge-potential relationships can also be described by:

$$\psi_o - \psi_\beta = \sigma_o / C_1 \qquad [1]$$

$$\psi_\beta - \psi_d = - \sigma_d / C_2 \qquad [2]$$

where C_1 and C_2 are the integral capacitances for the two regions as shown in Figure 19. An additional requirement is that overall electroneutrality must be maintained:

$$\sigma_o + \sigma_\beta + \sigma_d = 0, \qquad [3]$$

At equilibrium, the concentration of an ion in the interface can be tied to its concentration in the bulk solution by the Boltzmann distribution:

$$[j]_i = [j]\exp(-e\psi_i/kT) \qquad [4]$$

where $[j]_i$ represents the volume concentration of ion j which is at any plane i and experiencing potential ψ_i, and [j] represents its bulk concentration. Also, the relation between the total charge density inside the double layer, the potential ψ_d, and the bulk ionic concentrations is given by Gouy-Chapman theory:

$$\sigma_d = - \left[\frac{\epsilon CkT}{2\pi}\right]^{1/2} \sinh(ze\psi_d/2kT) \qquad [5]$$

where ϵ is the dielectric strength of the bulk fluid medium, and C is the total ionic strength in the supporting electrolyte. These concepts, and a knowldege of the equilibrium distribution of ions in the bulk fluid and in the interface, completely specify the relation between solution chemistry and double-layer chemistry.

4.1 Thermodynamics of the Hybrid-Site Interface

The interface is considered to contain one type of amphoteric group, MH, having N_A sites per unit area available for reaction with the acid HAn or base CtOH. The solid is suspended in a 1-1 electrolyte (CtAn) solution at known

concentration and pH. Seven primary surface reactions can occur at this amphoteric site:

$$MH_2^+ \rightleftharpoons MH + H_s^+ \qquad K_1 \qquad [6]$$

$$MH \rightleftharpoons M^- + H_s^+ \qquad K_2 \qquad [7]$$

$$MH_2^+ + An_s^- \rightleftharpoons MH_2An \qquad K_3 \qquad [8]$$

$$M^- + Ct_s^+ \rightleftharpoons MCt \qquad K_4 \qquad [9]$$

$$MHCt^+ \rightleftharpoons MH + Ct_s^+ \qquad K_5 \qquad [10]$$

$$MHAN^- \rightleftharpoons MH + An_s^- \qquad K_6 \qquad [11]$$

$$MHCtAn + H_s^+ \rightleftharpoons MH_2An + Ct_s^+ \qquad K_7 \qquad [12]$$

The first two reactions represent protonation and deprotonation of the amphoteric site, while the third and fourth show the primary complexation reactions. The fifth and sixth reactions represent specific adsorption of cations and anions onto neutral surface sites. The final reaction represents an ion exchange which does not affect the zeta potential.

To accomodate a second ionizable surface site, B, having N_B sites per unit area, we propose the additional reactions:

$$B + H_s^+ \rightleftharpoons BH^+ \qquad K_8 \qquad [13]$$

$$BHAn \rightleftharpoons BH^+ + An_s^- \qquad K_{10} \qquad [14]$$

$$BCt^+ \rightleftharpoons B + Ct_s^+ \qquad K_{12} \qquad [15]$$

$$BAn^- \rightleftharpoons B + An_s^- \qquad K_{13} \qquad [16]$$

$$BCtAn + H_s^+ \rightleftharpoons BHAn + Ct_s^+ \qquad K_{14} \qquad [17]$$

The first reaction here represents the protonation of the basic site B; the complementary deprotonation reaction will not occur. Similarly, the second reaction represents specific adsorption of anion on the positively charged BH^+ site. The final three equations parallel [10] - [12] above.

At equilibrium, the chemical potential of the surface and solution concentrations of each components must be equal. For the solution components (H^+, OH^-, Ct^+, An^-), the chemical potential is given by

$$\mu_j = \mu_j^o + RT \ln a_j \qquad [18]$$

where a_j, the activity of the jth component, is taken here to be the bulk concentration. For the surface groups (MH, MH_2^+, M^-, MH_2An, MCt, $MHCt^+$, $MHAn^-$, MHCtAn, B, BH^+, BHAn, BCt^+, BAn^-, BCtAn) the chemical potential is

$$\mu_{j,s} = \mu_{j,s}^o + zF\psi_j + RT \ln a_{j,s} \qquad [19]$$

where z is the charge on the site, ψ_j is the potential at the location of the particular group, F is Faraday's constant, and $a_{j,s}$ is the activity of the jth species on the surface, taken here to be the surface number density of the group. The term $zF\psi_j$ represents the work required to bring an ion from the bulk to the appropriate interfacial plane. The random-mixing approximation is used to estimate the activities of the surface components from their bulk concentrations. Using the notation $[\![i]\!]$ to represent the number density of surface species i, and [j] to represent the bulk concentration of an ion j in solution, the concentrations of the twelve possible surface complexes written in terms of the known bulk concentrations are:

$$[\![M^-]\!] = [\![MH]\!] K_2 Y / [H^+] \qquad [20]$$

$$[\![MH_2^+]\!] = [\![MH]\!] [H^+] / K_1 Y \qquad [21]$$

$$[\![MH_2An]\!] = [\![MH]\!] [H^+] [An^-] B / K_1 K_3 Y \qquad [22]$$

$$[\![MCt]\!] = [\![MH]\!] [Ct^+] K_2 Y / [H^+] K_4 B \qquad [23]$$

$$[\![MHCt^+]\!] = [\![MH]\!] [Ct^+] / K_5 B \qquad [24]$$

$$[\![MHAn^-]\!] = [\![MH]\!] [An^-] B / K_6 \qquad [25]$$

$$[\![MHCtAn]\!] = [\![MH]\!] [An^-] [Ct^+] / K_1 K_3 K_7 \qquad [26]$$

$$[\![BH^+]\!] = [\![B]\!]\,[H^+] \,/\, K_8\, Y \qquad [27]$$

$$[\![BHAn]\!] = [\![B]\!]\,[H^+]\,[An^+]\,B \,/\, K_8\, K_{10}\, Y \qquad [28]$$

$$[\![BCt^+]\!] = [\![B]\!]\,[Ct^+] \,/\, K_{12}\, B \qquad [29]$$

$$[\![BAn^-]\!] = [\![B]\!]\,[An^-]\,B \,/\, K_{13} \qquad [30]$$

$$[\![BCtAn]\!] = [\![B]\!]\,[An^-]\,[Ct^+] \,/\, K_8K_{10}K_{14} \qquad [31]$$

where

$$Y = \exp(e\psi_o/kT) \qquad [32]$$

$$B = \exp(e\psi_\beta/kT) \qquad [33]$$

and

$$N_A = [\![MH]\!]+[\![MH_2^+]\!]+[\![M^-]\!]+[\![MH_2An]\!]+[\![MCt]\!]+ [\![MHCt^+]\!]+[\![MHAn^-]\!]+[\![MHCtAn]\!] \qquad [34]$$

$$N_B = [\![B]\!]+[\![BH^+]\!]+[\![BHAn]\!]+[\![BAn^-]\!]+[\![BCt^+]\!]+[\![BCtAn]\!]. \qquad [35]$$

The relationship between ψ_o, ψ_β, ψ_d, C_1, C_2, σ_o, σ_β and σ_d are given by [1] - [3] while σ_o and $-\sigma_d$ are calculated from:

$$\sigma_o = e([\![MH_2^+]\!]-[\![M^-]\!]+[\![MH_2An]\!]-[\![MCt]\!]+[\![BH^+]\!]+[\![BHAn]\!]) \qquad [36]$$

$$-\sigma_d = e([\![MH_2An]\!]-[\![MCt]\!]+[\![MHCt^+]\!]-[\![MHAn^-]\!] +[\![BHAn]\!]+[\![BCt^+]\!]-[\![BAn^-]\!]). \qquad [37]$$

The values of σ_d are also obtained from [5] with

$$C = ([H^+] + [OH^-] + [Ct^+] + [An^-])/2 \qquad [38]$$

A Newton-Raphson calculation can be used to numerically solve this system of equations for the relation between surface charge and potential, the 12 complexation constants, the surface species concentrations, and bulk solution concentrations.

Unlike previous models, this model can allow for a sizable fraction of sites to be charged at the isoelectric point. Also, in fairly concentrated

suspension, complexation of charged surface sites could lead to substantial depletion of the available cation or anion available from the bulk solution. In order to account for adsorbed anion and cation, a second iteration algorithm can be superimposed on the Newton-Raphson calculation described above. The algorithm to correct the bulk salt concentration follows:

$$[Ct^+] = [Ct^+]^o - \lambda\,([\![MCt]\!] + [\![MHCt]\!] + [\![MHCtAn]\!] + [\![BCt]\!] + [\![BCtAn]\!]) \quad [39]$$

$$[An^-] = [An^-]^o - \lambda([\![MH_2An]\!] + [\![MHAn]\!] + [\![MHCtAn]\!] + [\![BHAn]\!] + [\![BAn]\!] + [\![BCtAn]\!]) \quad [40]$$

where $[\ ]^o$ is the ion concentration before addition of powder and λ is a conversion factor between surface concentration and volume concentration.

To increase the probability of convergence a third iteration procedure can be added to find ψ_β before calculating σ_d. Details of the numerical logic and the convergence criteria selected can be found in Reference 31. To avoid overprediction of adsorption at high (> 0.01 M) ionic strengths, we also found it necessary to include activity coefficients in the calculation determining surface chemical potentials from the concentration of bulk supporting electrolyte ions. This leads to substitution of activities for concentrations in [20] - [31]. Activities of the ions were determined from bulk concentrations and physical data for activity coefficients of each species at the bulk concentrations.

4.2 Implementation

For convenience in applying the model for the calculation of surface adsorption and zeta potential behavior, we use the following parameters:

$$pzc = (pK_1 + pK_2)/2, \quad \text{where } pK_j = -\log K_j \qquad [41]$$

$$\Delta pK = pK_2 - pK_1 \qquad [42]$$

$$G_j = 2.303\ pK_j = \Delta\mu_j^o/RT \quad \text{for } j=1,14. \qquad [43]$$

Thus, the G_j reported later are free energies of complexation in units of RT.

A non-linear regression algorithm[30] was used for determination of the 16 parameters (12 complexation constants, N_A, N_B, C_1, and C_2). The algorithm allows *a priori* assignment of up to 15 fixed parameters (i.e., parameters not altered during the course of the regression scheme). The necessary derivatives are numerically estimated since no explicit equation can be written to relate either the surface charge or the zeta potential to the 16 parameters. The regression routine modifies the step size and direction to obtain the benefits of both a steepest-descent approach to the optimum as well as requiring a small enough step size to uphold the accuracy of the linearity assumption implicit in the estimation of the partial derivatives.

Nevertheless, the algorithm can be unstable when all 16 parameters are entered with arbitrary starting values. To improve the probability of convergence at a physically plausible solution, it is necessary to carefully select the starting values for each parameter. In addition it is necessary to fix the values of parameters which are highly correlated (or otherwise have no assignable effect on the residuals) in order to achieve closure. Initial estimates for ΔpK, G_2, G_4, G_8, and G_{10} were obtained from double extrapolation estimates described below. The capacitances were fixed at the values which

James[19] chose for silica: C_1 = 125 $\mu C/cm^2$ and C_2 = 20 $\mu C/cm^2$. The bounds on N_A and N_B are established from experimental evidence: N_A and N_B must be greater than the maximum site densities observed during titration; and, the total number of sites is expected to be less than or equal to the site density of silanols on silica (4.6 sites/nm^2). G_7 and G_{14} were taken to be -20 RT as per Johnson[31]. Adsorption to uncharged amphoteric silicon nitride sites is assumed to be indistinguishable from adsorption to the basic site: ie. $G_5 = G_{12}$ and $G_6 = G_{13}$.

Extension of the extrapolation methods of Davis, James, and Leckie[28] can be accomplished by first rewriting the site-binding reactions as:

$$MH + Ct_s^+ \rightleftharpoons MCt + H_s^+ \qquad {}^*K_{Ct} \qquad [44]$$

$$B + H_s^+ + An_s^- \rightleftharpoons BHAn \qquad 1 / {}^*K_{An} \qquad [45]$$

so that

$${}^*K_{Ct} = K_2 K_4 \qquad [46]$$

$${}^*K_{An} = K_8 / K_{10} \qquad [47]$$

Assuming that surface complexation is negligible (very low ionic strengths), K_2 and K_8 can be estimated as follows:

$$pK_2 = pH - \log\left(\frac{\alpha^-}{1-\alpha^-}\right) + e\psi_o / 2.3\ kT$$

$$\equiv pQ_2 + e\psi_o / 2.3\ kT \qquad [48]$$

$$pK_8 = pH + \log\left(\frac{\alpha^+}{1-\alpha^+}\right) + e\psi_o / 2.3kT$$

$$\equiv pQ_1 + e\psi_o / 2.3\ kT \qquad [49]$$

where pQ_1 and pQ_2 are apparent acidity quotients evaluated from bulk solution concentrations and $pK_i = -\log_{10}(K_i)$. In these expressions, α^- and α^+ are the fractional surface charge:

$$\alpha^- = -\sigma_o / e(N_A + N_B), \text{ if } \sigma_o < 0 \qquad [50]$$

$$\alpha^+ = \sigma_o / e(N_A + N_B), \text{ if } \sigma_o > 0 \qquad [51]$$

where σ_o, the charge at the surface, and σ_β, the charge at the complexation plane, are given by:

$$\sigma_o = e([\![BH^+]\!] + [\![BHAn]\!] - [\![M^-]\!] - [\![MCt]\!]) \quad [52]$$

$$\sigma_\beta = e([\![BHAn]\!] + [\![MCt]\!]). \quad [53]$$

Numerical estimates of pK_2 and pK_8 are then obtained by plotting pQ_1 or pQ_2 vs the appropriate fractional ionization term, α^+ or α^-. At low ionic strengths, the intercept (pQ at $\alpha = 0$) should then be a good estimate of the acidity equilibrium constants at negligible complexation.

Likewise, an estimate of the complexation constants can be made using titration data taken at high ionic strength, where complexation can be expected to dominate. Assuming that surface complexation is now solely responsible for σ_o, then algebraic manipulation of [20], [23], [47], and [48] yields:

$$p^*K_{Ct} = pH - \log(\frac{\alpha^-}{1-\alpha^-}) + \log[Ct^+] + e(\psi_o-\psi_\beta)/2.3\ kT$$

$$\equiv p^*Q_{Ct} + e(\psi_o-\psi_\beta)/2.3\ kT \quad [54]$$

$$p^*K_{An} = pH + \log(\frac{\alpha^+}{1-\alpha^+}) - \log[An^-] + e(\psi_o-\psi_\beta)/2.3\ kT$$

$$\equiv p^*Q_{An} + e(\psi_o-\psi_\beta)/2.3\ kT \quad [55]$$

If there is no specific adsorption, then when $\sigma_o = 0$, $\psi_o = \psi_\beta$ and hence $p^*K = p^*Q$. Hence the intercept of a plot of p^*Q versus the appropriate fractional ionization, α, (ie. p^*Q at $\alpha = 0$) should be a good estimate of p^*K for systems where the ionic strength is high enough that complexation dominates the surface charge behavior.

To improve upon these estimates, James and Parks[19] suggest a double extrapolation technique whereby one can estimate pK_2 and pK_8 at infinite dilution from a plot of pQ vs $(\alpha + [CtAn]^{0.5})$ and estimate p^*K_{Ct} and p^*K_{An} at infinite salt concentration from a plot of pQ vs $(\alpha - \log[CtAn])$.

Further improvement in the starting values for the regression parameters was obtained by a stepping routine which was able to survey broad regions of the parameter space. For each parameter set, the standard error (square root of the sum of squares of residuals divided by the degrees of freedom) was evaluated. Also, plots allowed visual determination of the goodness of fit and the appropriate direction to search for a better fit.

4.3 Application of the Model to Silicon Nitride Dispersions

Table 1 shows the standard error obtained when surface charge and potential are predicted by inserting the parameters obtained from the double extrapolation analysis directly into the hybrid-site model. The error in predicting surface charge and potential in comparison to the experimentally observed values is also reported. Figure 20 graphically compares these predictions to experimental observation.

Results of the stepping routine for the starting parameters for the regression analysis of the hybrid-site model are given in Table 2. The final parameter values, along with the starting conditions and constraints utilized in the regression routine, are also listed. Figures 21 and 22 show the predicted surface charge and zeta potential for UBE silicon nitride. For comparison, the model parameters, which were obtained using data taken at 0.001 M and 0.01M KNO_3, were used to predict surface charge for higher ionic strengths as well.

4.4 Discussion

As can be seen in Table 2, titration data alone, even at several ionic strengths, does not yield enough information to uniquely define all 16

parameters. Acceptable fits can be obtained with the various parameter sets listed. The additional constraint of requiring the model to also predict electrophoresis data improves the situation somewhat, but does not resolve the problem. Specifically, we have found a high correlation between the acid/base dissociation constants (K_1, K_2, K_8) and the constants describing complexation to the charged sites (K_4, K_{10}). We have found that complexation to uncharged sites (K_5, K_6) has such a small effect on the surface charge and is so highly correlated to both the dissociation and the complexation phenomena above that these constants cannot be found using the regression scheme. The number of surface sites (N_A and N_B) is also highly correlated with the equilibrium constants, and it was necessary to fix these parameters at plausible values in order to estimate the remaining parameters.

The predicted surface charge was most sensitive to pK_2 and pK_8 (the active acid and base site adsorption constants). Changes as small as 1 pK unit are significant because these two parameters strongly influence the pH where the inflection points in the titration data occur. Salt complexation constants have a secondary effect on the pH at which the inflection points occur. The number of surface sites most strongly affects the magnitude of the site density when the surface charge plateaus at either high or low pH. Unequal energies for cations and anions adsorbing to uncharged sites allows the isoelectric point to occur at a different pH from the pzc. Relatively large changes in the adsorption free energy at these sites (2-3 RT) are necessary to produce a noticable effect on the regression error.

The titration curves for silicon nitride suggest that either the silanol site density is greatly reduced below that of silica or the acidity of the

silicon nitride silanol is lower than that of silanols found on pure silica. However, Busca[8] observed that the silanol sites on his amorphous silicon nitride were less acidic than silanols on silica. Hence, since it was impossible to predetermine either the silanol site density or pK α *priori*, both parameters were allowed to float in the regression analysis. The total site density was maintained at approximately 5 sites/nm^2 under the assumption that the surface structure is a substituted silica. It was still possible to find many plausible sets of parameters which fit the titration data equally well (have equivalent sum-of-squares error). Goodness-of-fit to electrophoresis data helps eliminate some parameter sets, but does not produce a unique set.

Exact coincidence of ionization constants estimated from the double extrapolation method and the regression scheme cannot be expected. The double extrapolation method does not account for specific adsorption of supporting electrolyte ions to uncharged surface sites nor does it allow for significantionization of the surface sites at the pzc. The latter simplification was expected to be insignificant for silica and its analogues since Healy and White[17] predicted that the number of positive and negative charged surface sites existing at the pzc will be negligible for species with Δpk above 6. We also explicitly based our modified double extrapolation method for silicon nitride on this assumption. On the other hand, specific adsorption to uncharged sites appears to play an important role for silica, and should, by analogy, for silicon nitride. The almost linearly increasing zeta potentials obtained by Wiese[32], Li[33], and Hunter[34] for silica at low pH (where the proton adsorption measured by titration remains negligible) suggests that the electrolyte complexes with surface sites. Finally, the persistent minima in the double extrapolation plots of α vs

pQ or p^*Q suggest that ψ_β does not equal ψ_o at α (or H^+ adsorption) equals zero.

These problems have been manifest in earlier attempts by Yates[35] to apply this site model to silica. Yates found that the silica electrophoresis curves fit, somewhat poorly, a model assuming $\Delta pK = 6$, while the titration data fit a model which assumed $\Delta pK = 10$. Although Yates recognized the possibility of complexation of supporting electrolyte ions in the development of the double layer, he did not include them in his calculations which is perhaps the reason he was unable to resolve this discrepancy. Wiese[18] included complexation in their model calculations and did not observe this discrepancy in qualitative analysis comparing electrophoresis results to the model, but did not report attempts to quantitatively predict either electrophoresis or titration experiment results.

As discussed earlier, the number of sites present on the surface of silica has been reported frequently in the literature, and a value between 4.6 and 5 sites/nm^2 appears to be representative of all silicas, be they crystalline or amorphous. The distribution of ionizable silanols and non-participatory siloxanes, as well as the distribution of hydrogen-bonded vs. free silanols appears to vary dramatically depending upon the conditions of formation of the surface sites. Although a fully hydroxylated surface appears to contain a full complement of silanols (4.6-5 sites/nm^2), only two-thirds of these silanols appear to protonate in aqueous environments. James[19] attributes this limit to the accumulation of surface charge preventing full ionization of the surface species; Armistead[11] predicts that the acidity of hydrogen-bonded and non-hydrogen bonded silanols will be different, and two different pK's might better describe silica interfacial chemistry.

We suspect that three equilibrium constants may be necessary to fully describe the system. Deprotonation of the first hydrogen-bonded silanol should occur most rapidly, followed closely by deprotonation of the free silanols. Deprotonation of the second hydrogen-bonded silanol (ca. 1.6 sites/nm^2) would appear very difficult since the final proton is now shared between the two hydrogen bonded sites as is the extra electron from the negatively charged silanol. Hence, one observes deprotonation of only one half of the hydrogen-bonded sites (1.6 sites/nm^2) plus deprotonation of all of the free silanols (1.6 sites/nm^2).

An additional simplification of the model is the assumption of constant capacitance. This assumption cannot be defended based on physical intuition, rather, it has been adopted because it provides a reasonable fit to titration data for several oxide systems. In contrast, Carnie's "Civilized Model" of the double layer[36] suggests that constant capacitance over a wide range of surface charge and ionic strength is more likely to be the exception than the rule. James[30] notes that his model only predicts diffuse potentials (ψ_d) which are equal to observed zeta potentials in a narrow pH range of 1 - 2 pH units on either side of the iep. This indicates that the location of the diffuse potential surface and the location of the zeta potential plane are diverging as the surface charge increases. The location of the diffuse potential is essentially set by the magnitude of the capacitances (C_1 and C_2); the location of the zeta potential is established by hydrodynamics. Hence it is more likely that, if the model accurately represents all other phenomena, the capacitances are not constant. Indeed, Johnson's model[31], which does not enforce the constant capacitance condition, is able to predict zeta potentials with good

success over a wide pH range. Despite all these potential sources of discrepancy, the hybrid-site model develped here provides semi-quantitative agreement with the exerimental results for silicon nitride dispersions. Successfull application of the model to silicon carbide dispersions has also been accomplished[29].

5. Conclusions

The aqueous colloidal chemistry of both silicon carbide and silicon nitride powders are governed by silanol surface functionalities. Additionally, silicon nitride powders, as received from the manufacturers, possess varying amounts of a second amine surface group, which can be removed or reduced in concentration by relatively mild pretreatments. The amount of this second surface group apparently depends on the powder synthesis route as well as the storage and handling conditions.

Comparison of the titration results of treated silicon nitride powders from various manufacturers reveals only minor differences relative proton adsorption/desorption from aqueous solution. The results of titration studies reveal a stong similarity to the proton uptake behavior of silicon carbide and silicon dioxide materials. The presence of ammonium ions in solution does not appear to influence the interfacial complexation reactions with proton or hydroxyl in solution. The results of titration studies also show qualitative agreement with observations of electrokinetic behavior.

Development of the double-layer model for the hybrid-site interface provides a means to understand and predict the surface complexation reactions that can take placce on silicon nitride powders. The intrinsic acidity of the silanol functionalities on silicon nitride and silicon carbide are found to be different from those on silica. In general, the silanols on silicon carbide are more acidic than those on silica, which are, in turn, more acidic than the silanols on silicon nitride.

Further studies, involving a more comprehensive examination of slip rheology and particle compaction behavior will be necessary to evaluate the accuracy of the interfacial model, or the utility of the pretreatment and modification strategies in improving processing characteristics for these materials.

Acknowledgements

The research described here is largely the work of three graduate students, P.K. Whitman, M.J. Crimp, and A.M. Thuer.

REFERENCES

[1] Quackenbush, C.,French, K., Neil, J.,"Fabrication of Sinterable Silicon Nitride by Injection Molding," presented at the Automotive Technology Development Contractor Coordination Meeting, Hyatt-Regency, Dearborn Michigan (Oct. 26-29, 1981).

[2] Reed, J., Carbone, C., Scott, C.,Lukasiewicz, S., Processing of Crystalline Ceramics, Materials Science Research Volume 11, ed. H. Palmour III, et.al, Plenum Press, New York (1978).

[3] Pasto, A., Quackenbush, C., French, K., Neil, J., in Ultrastructure Processing of Ceramics, Glass, and Composites, ed. R. Ulrich and L.L.Hench, Wiley, New York,p. 476 (1984).

[4] Lange, F. J. Am. Cer. Soc. **67(**2), 83 (1984).

[5] Mizuta, S., Cannon, W., Bleier, A., Haggerty, J., Am. Cer. Soc. Bull. **61**, 872 (1982).

[6] Irene, E., Ghez, R., Proceedings of the Third International Symposium on Silicon Materials Science and Technology, ed. H. Huff and E. Surtl, The Electrochemical Sociey, (1977).

[7] Rahaman, M., Boiteux, Y., De Jonghe, C., Am. Ceramic Soc. Bull. **65(**8), 1171 (1986)

[8] Busca, G., Lorenzelli, V, Porcile, G., Baraton, M., Quintard, P., Marchand, R., Materials Chem. and Phys.**14**, 123 (1986).

[9] Crimp, M.J., M. S. Thesis, Case Western Reserve University (1986).

[10] Iler, R., The Chemistry of Silica, John Wiley, New York 3-104 (1979).

[11] Armistead, C., Tyler, A., Hambleton, F., Mitchell, S., Hockey, J., J. Phys. Chem. **73**(11), 3947 (1969).

[12] Yates, D., Healy, T. , J. Colloid Interface Sci. **55**(1), 9 (1976).

[13] Bastik, J., C. R. Acad. Sci. **247**, 203 (1958).

[14] Kiselev, A. Adsorption, USSR Academy of Sciences, Moscow (1959).

[15] Boyle, T., Gaw, W., J. Chem.Soc. **1965**, 240, (1965).

[16] Bliznakov, G., Polikaarova, R., J. Catalysis **5**, 18 (1966).

[17] Healy, T., White, D., Adv. Colloid Interface Sci. **9**, 303 (1978).

[18] Wiese, G., James, R., Yates, D., Healy, T., MTP Int. Rev. Sci., Electrochem. Phys. Chem. Ser. 2, **6**, 52 (1976).

[19] James, R., Parks, G., Surface Colloid Sci., Vol. 12, 119 (1982).

[20] Overbeek, J., Colloid Science, Vol. 1, ed. H. Kruyt (1952).

[21] Parks, B., Bruyn, P., J. Phys. Chem. **66**, 967 (1962).

[22] Bowen, P., Carnegie Mellon University, personal comm.

[23] Aksay, I., Ambarian, C., "Development of Homogeneity in Si_3N_4 Ceramics by Colloidal Consolidation," prepared for Garett Turbine Engine Company, final report for work performed under P.O. #1800433, 6/83 to 9/83 (published 1984).

[24] Crimp, M., Johnson, R., Halloran, J., and Feke, D., in Ultrastructure Processing of Ceramics, Glasses, andComposites: Proceedings of the Second International Conference, ed. L. Hench and D. Ulrich, Chapter 56, Wiley (1986).

[25] Clark, D., Shaw, T., "Sintering Phenomena of Non-Oxide Silicon Compounds," TR4, Rockwell Intl. Sci. Center, 1000 Oaks CA, for period 1/82 through 12/82, DOE Contract DE-AC03-78 ERO 1885.

[26] "Improved Silicon Nitride for Advanced Heat Engines," Annual Tehnical Report No. 1, AiResearch Casting Co., for period 9/26/84 through 9/30/85, NASA CR-175006.

[27] Johnson, R., E. I. DuPont Co., Experiment Research Station, personal communication.

[28] Davis, J., James, R., Leckie, J., J. Colloid Interface Sci. **63**, 480 (1981).

[29] Whitman, P.K., "Colloidal Characterization of Ultra-Fine Silicon Nitride and Silicon Carbide Ceramic Powders", Ph.D. Dissertation, Case Western Reserve Univerisity, 1987.

[30] Marquardt, D., J. Soc. Ind. Appl. Math. **11**, 431 (1963).

[31] Johnson, R.E., J. Colloid Interface Sci., **100**(2), 540 (1984).

[32] Wiese, G., James, R. Healy, T., Disc. of Faraday Soc. **52**, 302 (1971).

[33] Li, H., DeBruyn, P., Surf. Sci. **5**, 203 (1966).

[34] Hunter, R., Wright, H., J. Colloid Interface Sci. **37**, 564 (1971).

[35] Yates, D., Levine, S., Healy, T., J. Chem. Soc., Faraday Trans I **70**, 1807 (1974).

[36] Carnie, S., Chan, D., Adv. Colloid Interface Sci. **16**, 81 (1982).

TABLE 1: Summary of Regression Model Fit Using Parameters from Double Extrapolation Analysis[M]

MATERIAL	N_A	N_B	pzc	ApK	C_3	C_4	C_5	C_6	C_7	C_8	C_9	C_{10}	C_{11}	C_{12}	C_{13}	C_{14}	C_1[f]	C_2[f]	SE_1[g]	SE_2[g]
UBE Si_3N_4 [a]	3.5	0.5	3.0	11.0	0.0	1.6	-20	-20	-20	8.5	n.a.	1.3	n.a	-20	-20	-20	125	20	0.18	16.5
UBE Si_3N_4 [b]	3.5	0.75	3.0	11.6	0.0	2.3	-20	-20	-20	8.6	n.a	1.2	n.a	-20	-20	-20	125	20	0 33	n.a.
Cabosil[c]	4.8	0.0	3.0	8.4	0.0	1.2	-20	-20	-20	n.a.	n.a.	n.a.	n.a.	n.a	n.a.	n.a.	125	20	0.33	n.a.
Cabosil[c]	4.8	0.0	3.0	8.4	0.0	2.1	-20	-20	-20	n.a.	n.a.	n.a.	n.a.	n.a	n.a.	n.a.	125	20	0.67	n.a.
Cabosil[c]	3.5	0.0	3.0.	8.8	0.0	3.2	-20	-20	-20	n,a.	n.a.	n.a.	n.a.	n.a	n.a.	n.a.	125	20	0.66	n.a.

[M] regression fit is for 0.001M and 0.01M KNO_3 data unless otherwise noted.

[a] raw, pretreated powder; [b] milled,pretreated powder; [c] fit to untreated M-5 data using 0.01M data only

TABLE 2: Summary of Intrinsic Ionization Constants Derived for Raw UBE Silicon Nitride.*

A. Fit using stepping routine (all parameters "fixed"):

Standard Error$_1$[b]	N_A	N_B	pzc	ApK	C_3	C_4	C_5	C_6	C_7	C_8	C_9	C_{10}	C_{11}	C_{12}	C_{13}	C_{14}	C_1[b]	C_2[b]	SE_2[c]
0.02133	2.8	0.5	3.0	10.0	0	0	0.5	0	-20	9.0	-20	0.5.	-20	0.5	0.5	0	125	20	17.7
0.0407	2.0	1.0	3.0	9.4	-5	-2	-5	-5	-20	9.4	-20	1.0	-20	-5	-5	-20	125	20	23.2
0.0504	2.8	0.5	3.0	10.3	0	0.5	0	0	-20	9.5	-20	0.5	-20	0	0	-20	125	20	17.8
0.0287	2.8	0.5	3.0	11.0	0	0	0	0	-20	10.0	-20	0.0	-20	0	0	-20	125	20	16.4

B. Fit using nonlinear least squares regression routine*

0.0214[d]	**1.64**	**1.86**	3.0	**9.52**	-5	**0.36**	0	0	-20	**7.88**	-20	1.0	-20	0	0	-20	125	20	18.0
0.0274	**2.98**	**0.52**	3.0	**10.0**	0	0	0	-5	-20	**9.59**	-20	0	-20	0	0	-20	125	20	n.c.
0.0260	**2.97**	**0.53**	3.0	**6.03**	-5	**3.41**	-5	-5	-20	**9.07**	-20	1.0	-20	-5	-5	-20	125	20	n.c.
0.0228	**2.23**	**1.27**	3.0	**9.06**	-5	**-1.50**	-5	-5	-20	**8.59**	-20	**-0.16**	-20	-5	-5	-20	125	20	n.c.
0.0225	**2.28**	**1.22**	3.0	**9.08**	-5	**-1.54**	-5	-5	-20	**8.44**	-20	1.0	-20	-5	-5	-20	125	20	n.c.

*regression fit is for 0.001M and 0.01M KNO_3 data unless otherwise noted; **bold** parameters are those which were fit by regression scheme (others were "fixed"); the sum of $N_A + N_B$ was always constrained to 3.5; n.c. is not calculated.

[a]SE_1 is standard error for σ_o (sites/nm^2); [b]C_1 and C_2 are $\mu C/cm^2$; [c]SE_2 is standard error of fit for ζ (mv); [d]plotted in Figure 4 and 5.

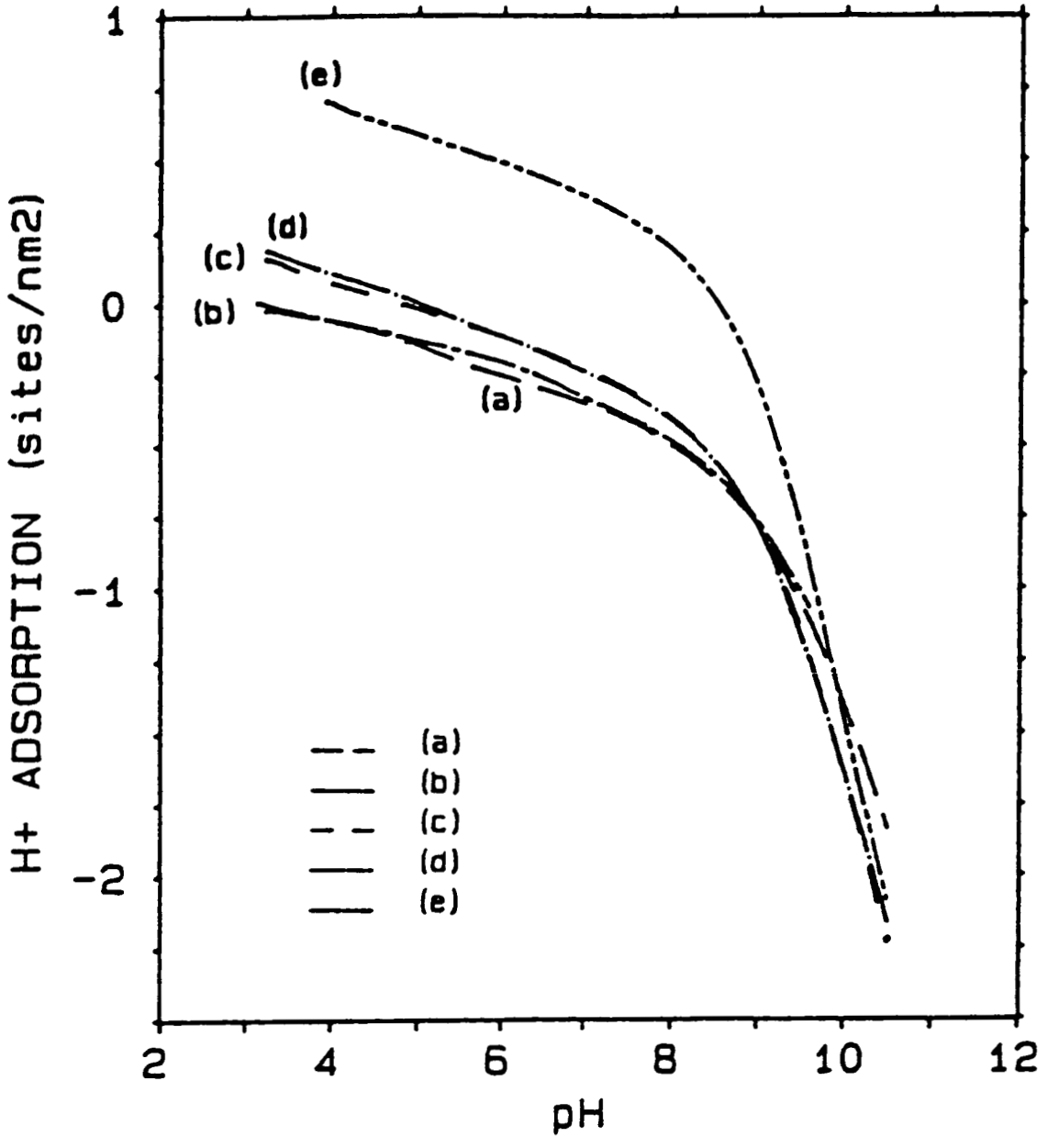

Figure 1

Comparison of the effect of pretreatment strategies on titration results of UBE silicon nitride: (e) as received powder; (d) and (c) powder moderately cleaned by vacuum treatment alone; (a) powder exposed to vacuum and acidified electrolyte washes; (b) titration results of curve (c) corrected by using centrate as reference liquid instead of pure electrolyte. Note the equivalent results obtained for well-cleaned powder and by compensating for titratable dissolved species in the centrate.

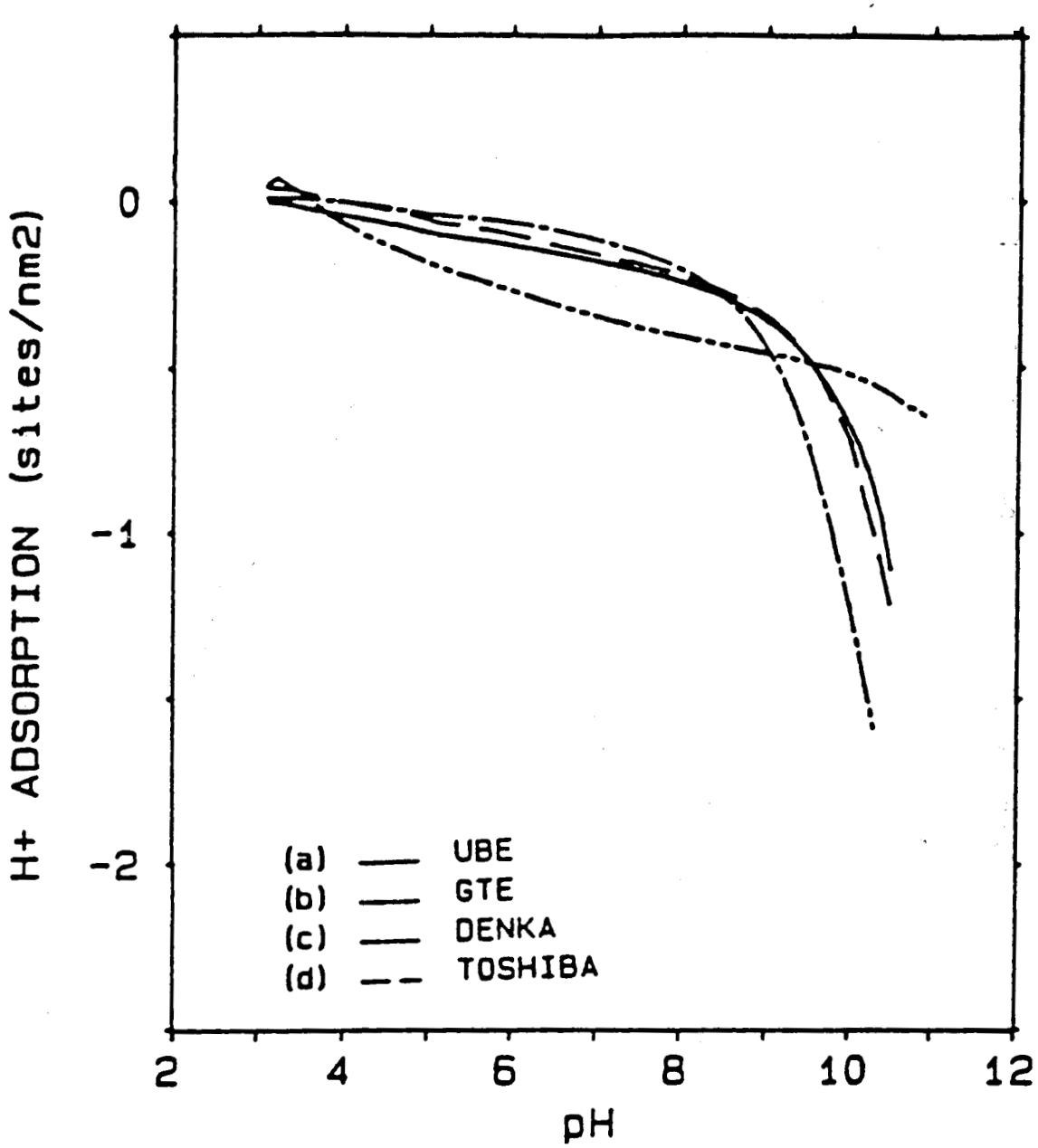

Figure 2

Comparison of the relative adsorption titration curves for silicon nitride powders produced by four different manufacturing methods. All powders were titrated in 0.001 M KNO_3 starting from pH 3. Note the similarity between curves (a), (b), and (d) at low pH and between (a) and (d) at high pH.

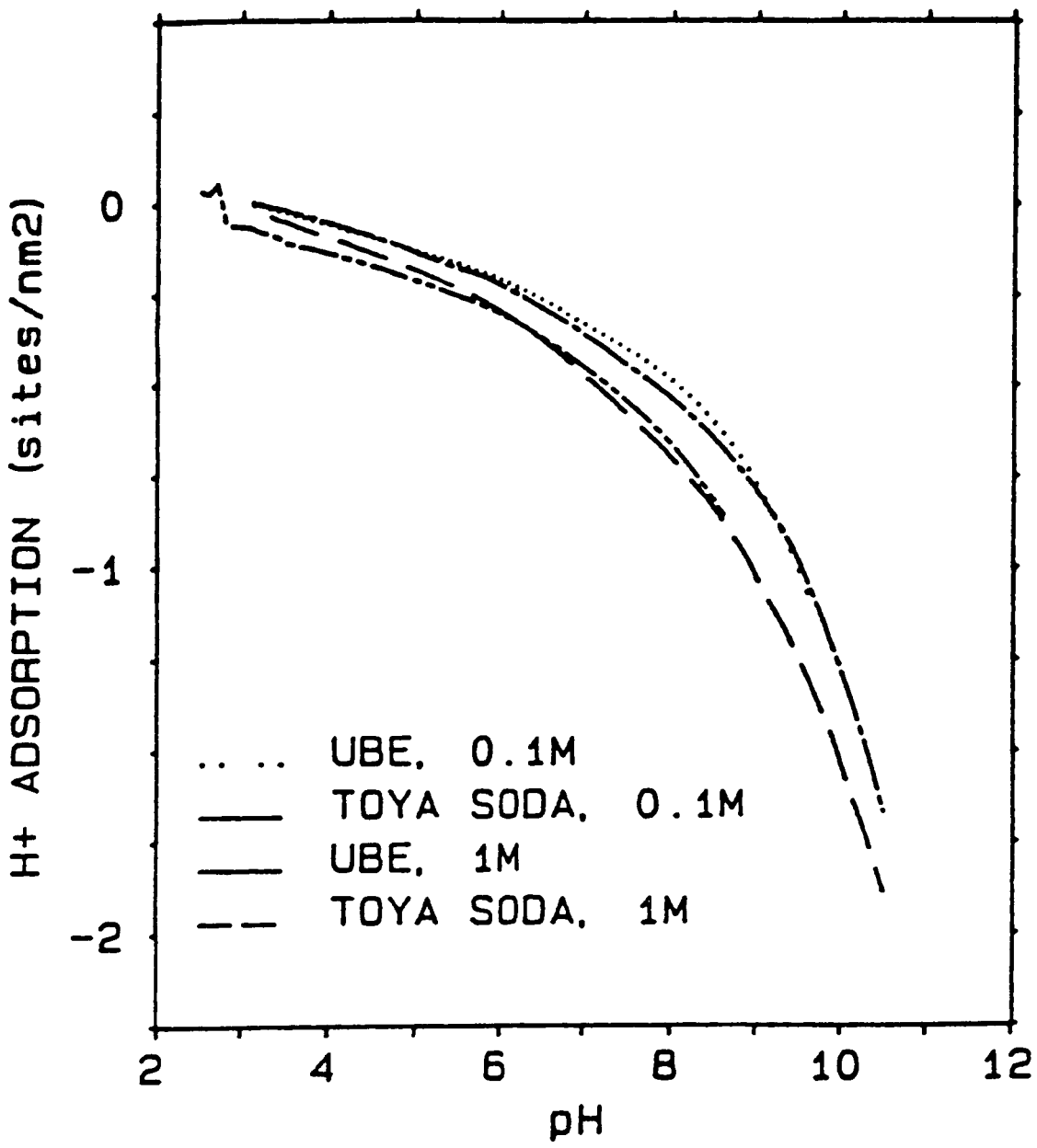

Figure 3

Comparison of titration results for well-cleaned UBE and Toya Soda powders in 0.1 M and 1 M KNO_3 electrolyte. These two powders are manufactured by two different suppliers who use the same basic manufacturing process.

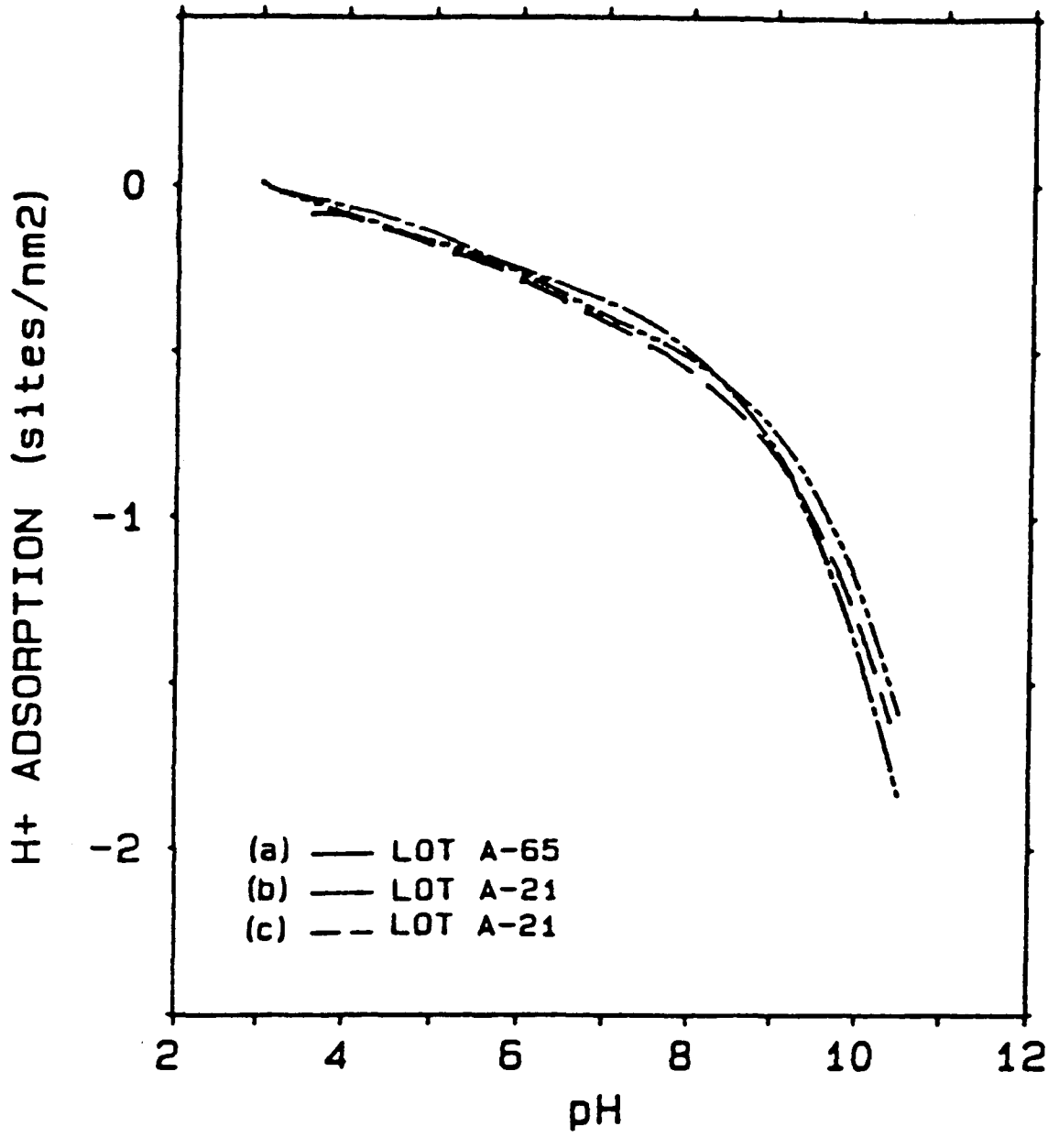

Figure 4

Comparison of relative adsorption titration curves for UBE silicon nitride from two different manufacturing lots: A-21 and A-65. All samples were titrated in 0.1 M KNO_3 solutions starting at pH 3. Curves (a) and (b) were washed in acidified electrolyte. Curve (c) was calculated using centrate for this DI water-washed, Ar dried sample.

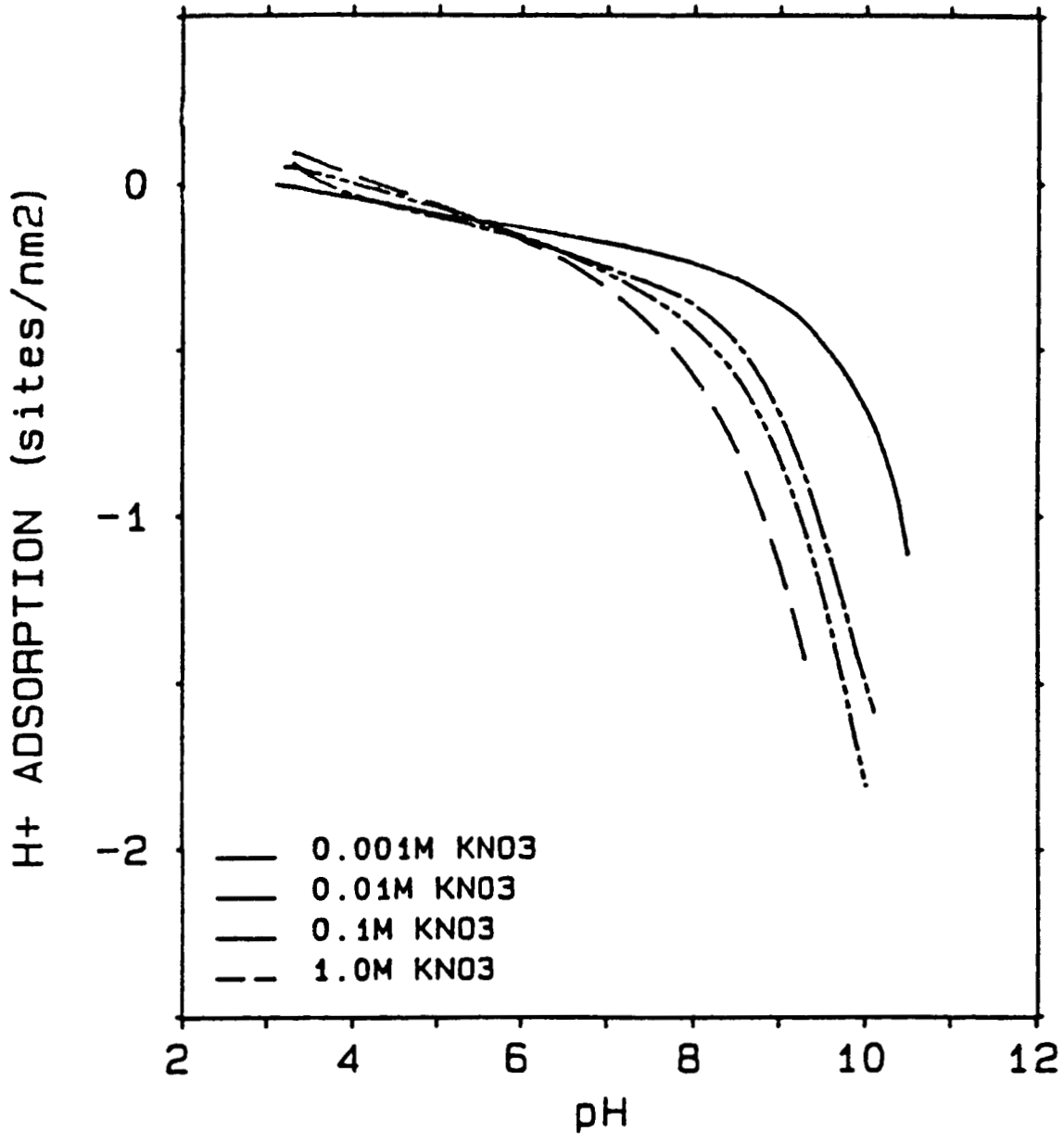

Figure 5

Relative adsorption titration curves for pretreated UBE silicon nitride powder in KNO_3 solutions of increasing ionic strength. Titration began at pH 3 in 0.001 M electrolyte and concluded back at pH 3 in 1 M solution. Note the cip which occurs at pH 5.6.

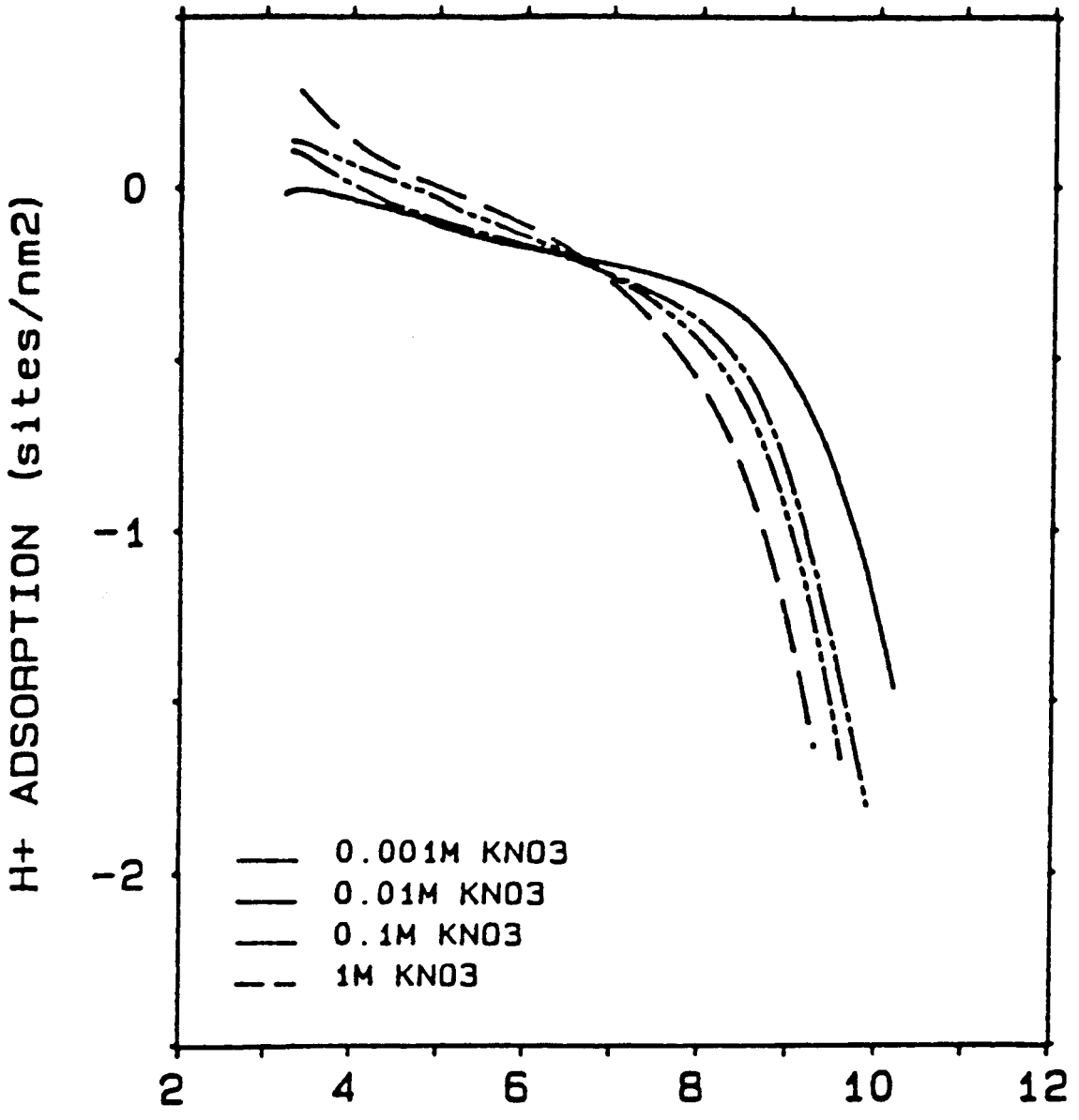

Figure 6

UBE silicon nitride powder which received only the vacuum pretreatment (no acidic electrolyte wash). Notice that a sharp cip still occurs, but that it is shifted to higher pH than the cip for acid-washed UBE silicon nitride.

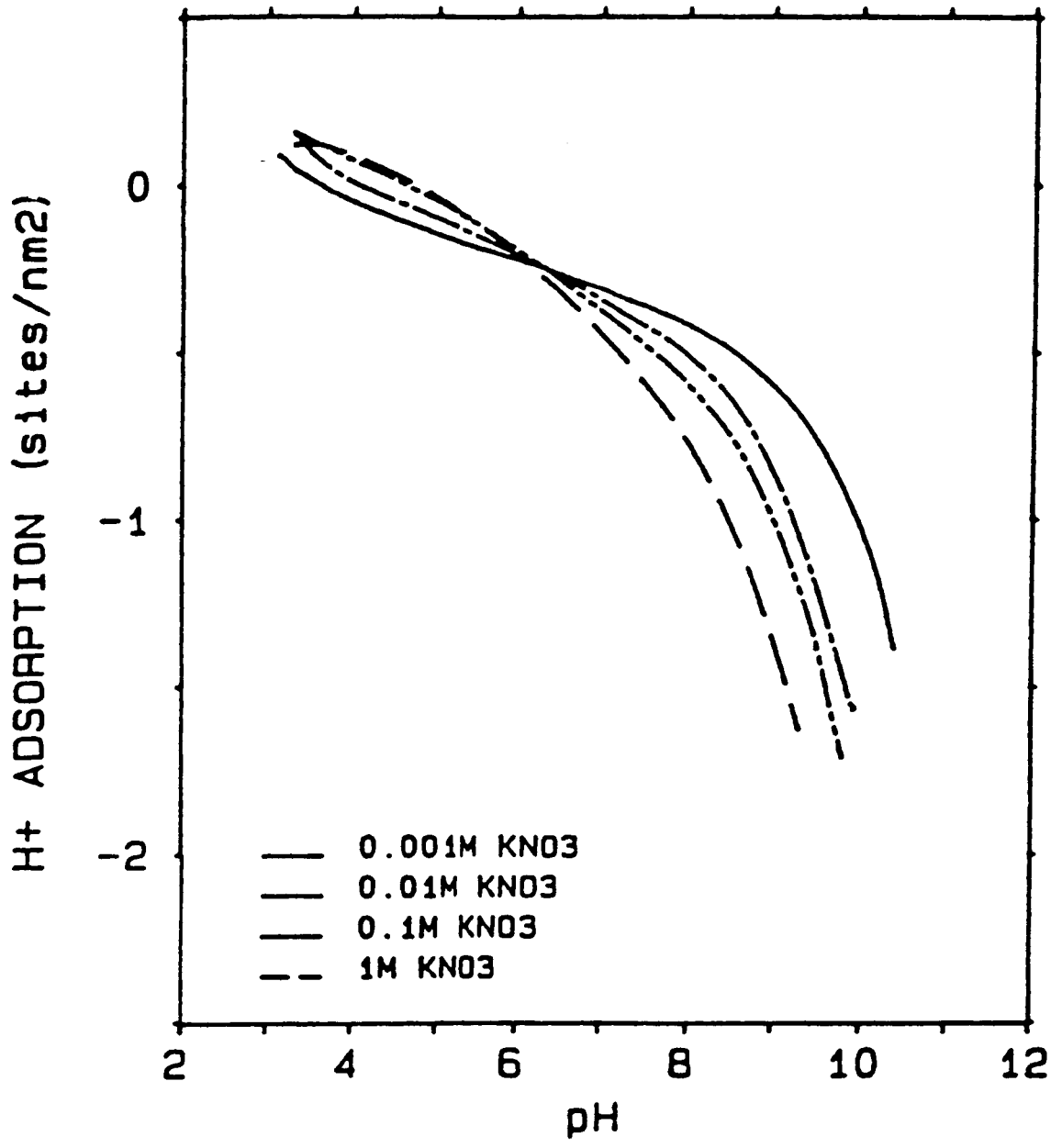

Figure 7

Well-washed (4 washes in 0.1 M KNO_3) milled UBE silicon nitride powder titrated in increasing ionic strength KNO_3 solutions. Notice the sharp cip which occurs at pH 6.2 and the increased proton adsorption at lower pH than is observed for raw (unmilled) UBE.

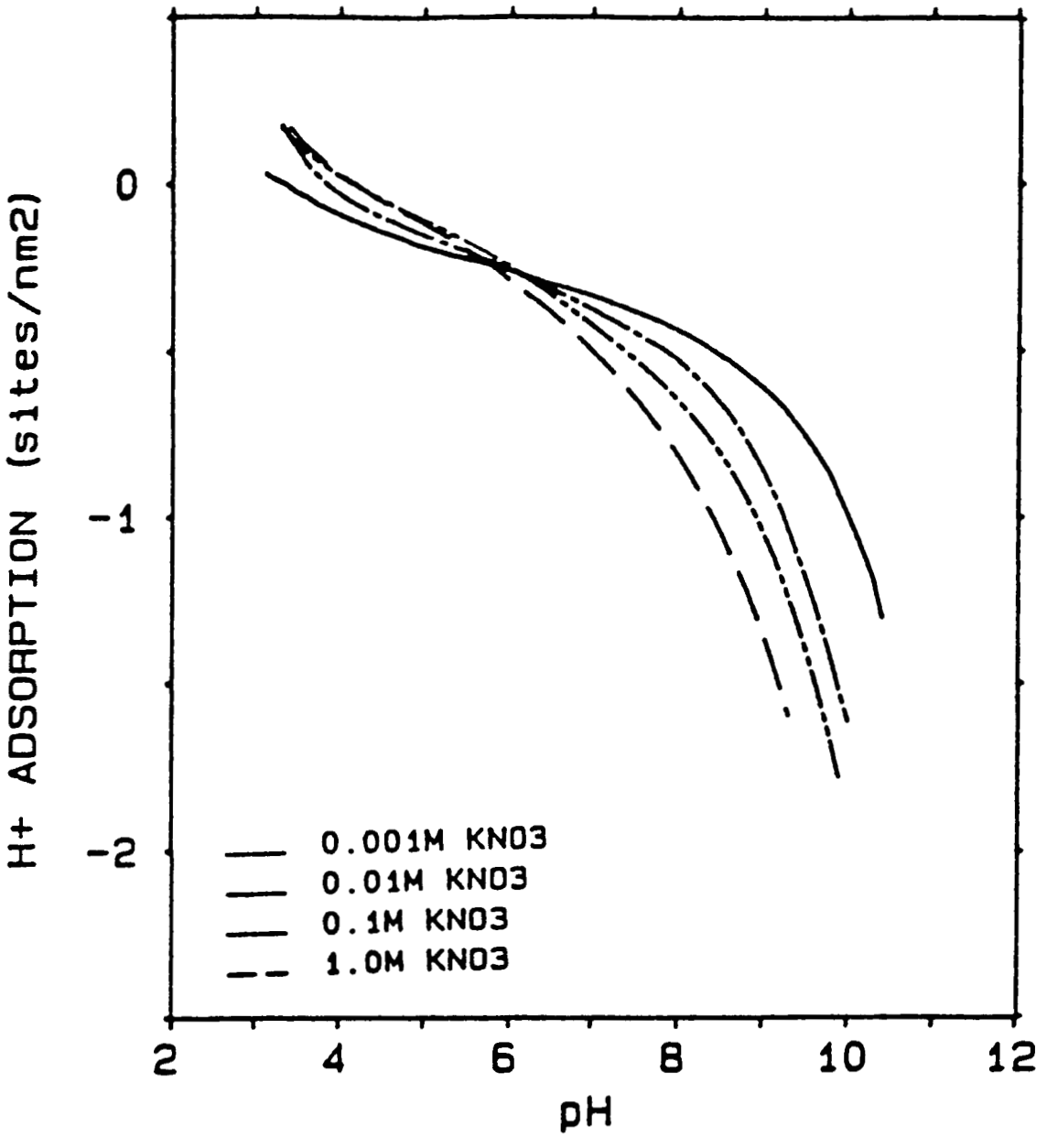

Figure 8

Well-washed milled UBE silicon nitride powder titrated in increasing ionic strength KNO_3 solutions. This powders was washed 11 times in 0.1 M KNO_3 after milling. Once again, the cip occurs at pH 6.2.

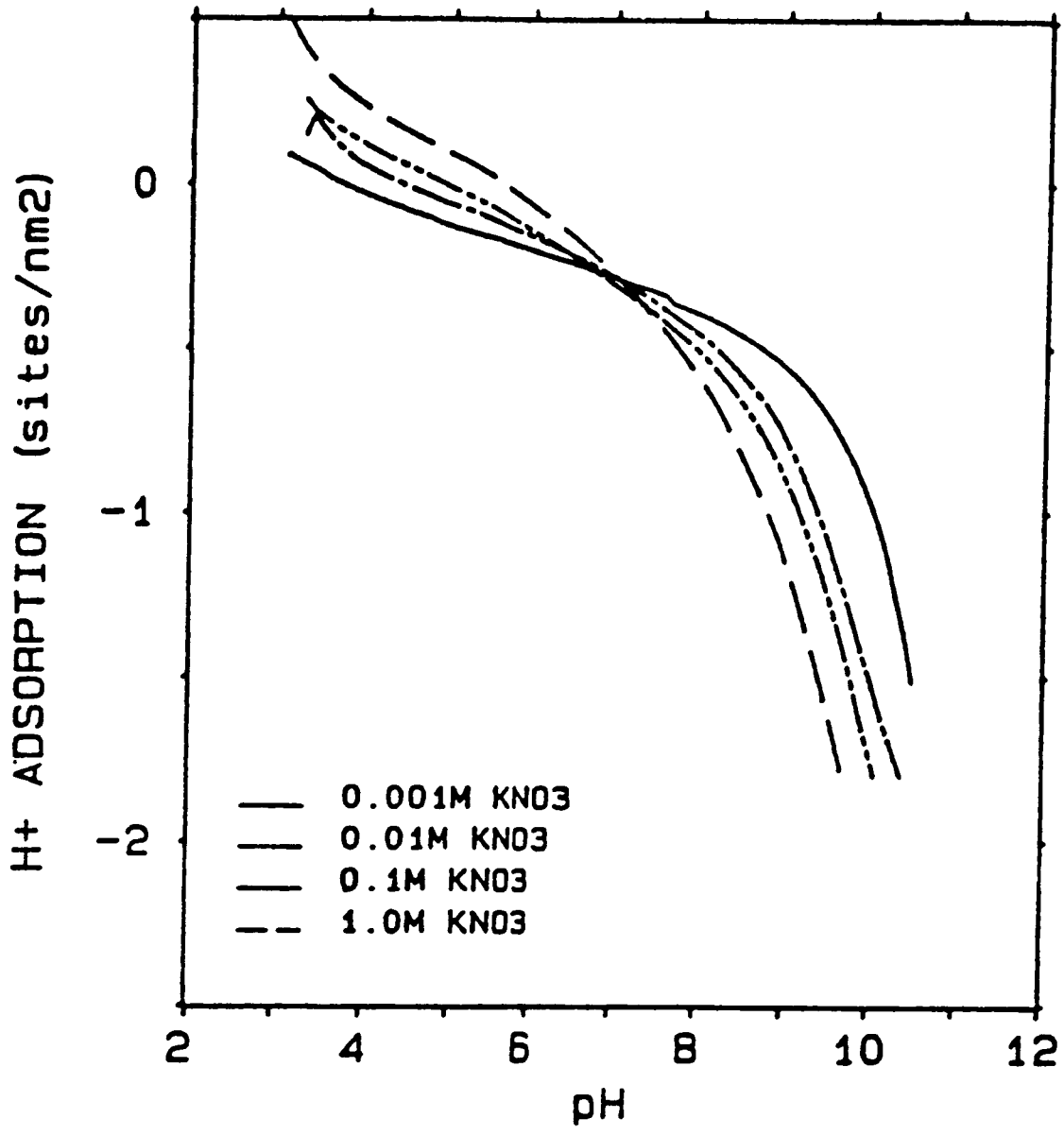

Figure 9

Partially cleaned milled UBE silicon nitride powder titrated in increasing ionic strength KNO_3 solutions. This sample was washed 3 times in 0.001 M KNO_3 solution before refilling and titrating in 0.001 M KNO_3. Note the cip at pH 6.5 --which is higher pH than the cip for well-washed milled UBE powders (Figures 7 and 8).

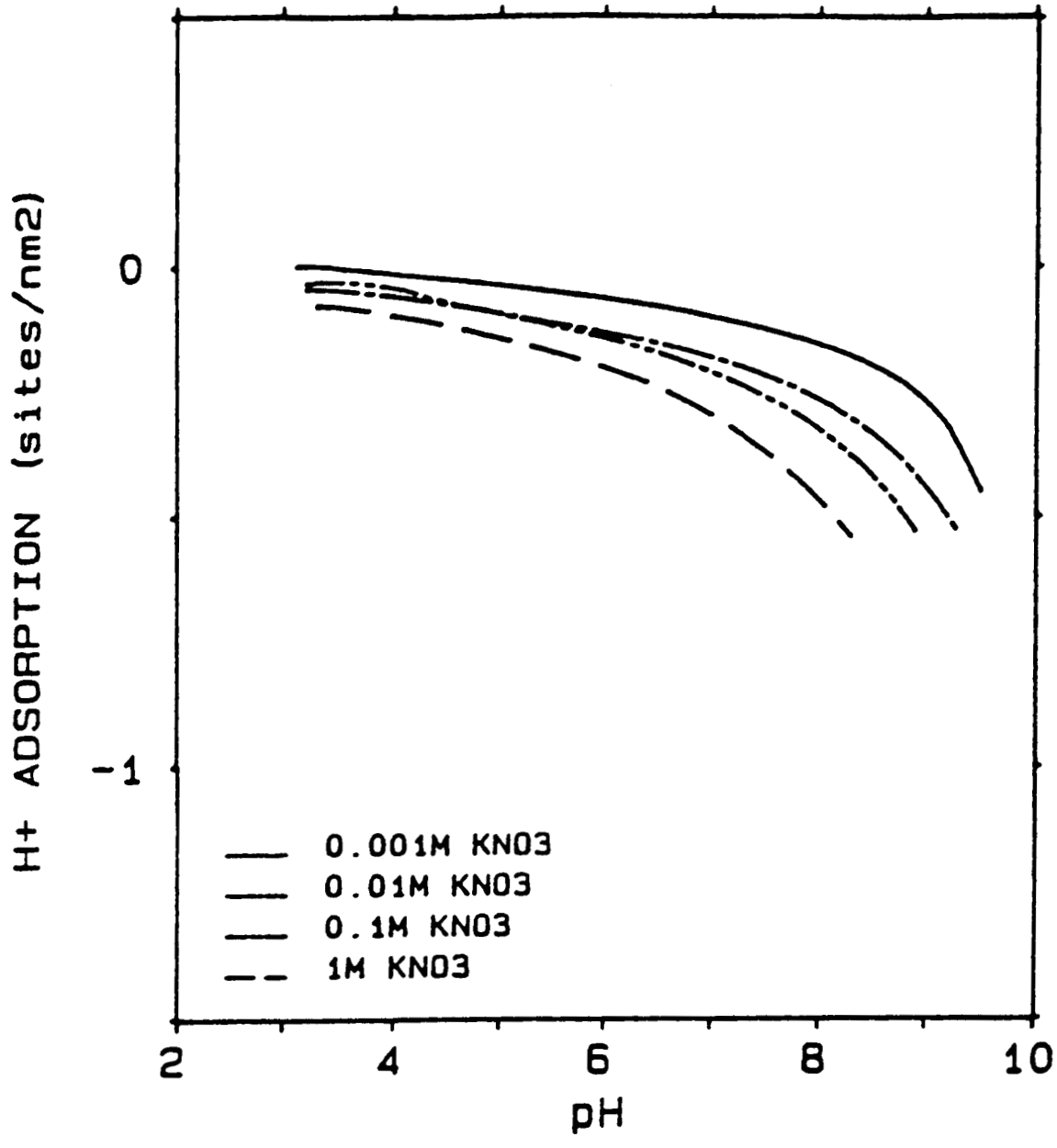

Figure 10

Relative adsorption titration curves for pretreated Lonza UF-15 silicon carbide powder in KNO_3 solutions of increasing ionic strength. Titration began at pH 3 in 0.001 M electrolyte and concluded back at pH 3 in 1 M solution. Note that no obvious cip occurs in the pH region explored.

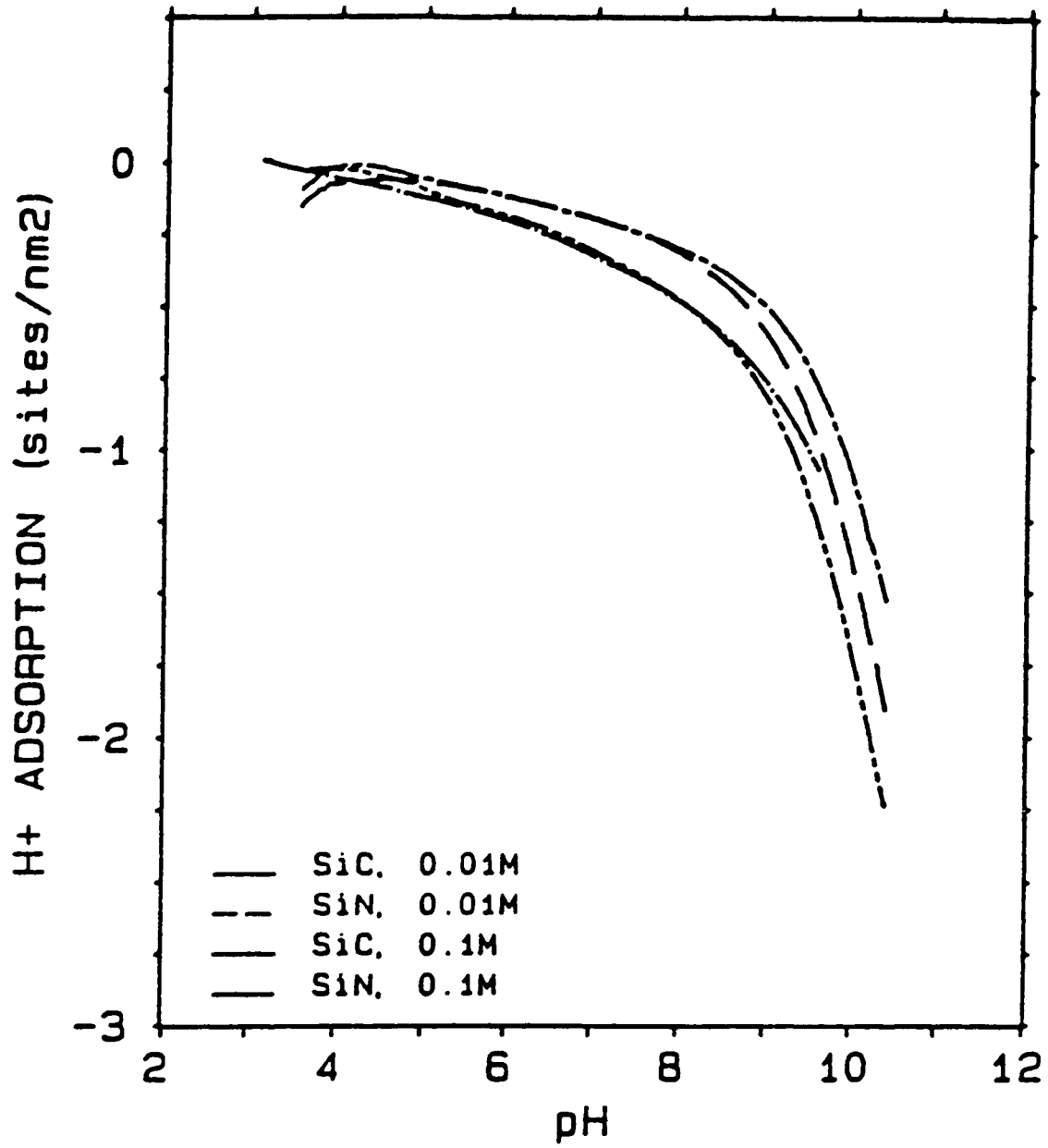

Figure 11

Titration profiles for well-cleaned UBE silicon nitride and Lonza silicon carbide powders. Upper curves were obtained at low ionic strength (0.01 M KNO_3) while lower curves were obtained at higher electrolyte concentration (0.10 M KNO_3). Note the similarity between the results for each material.

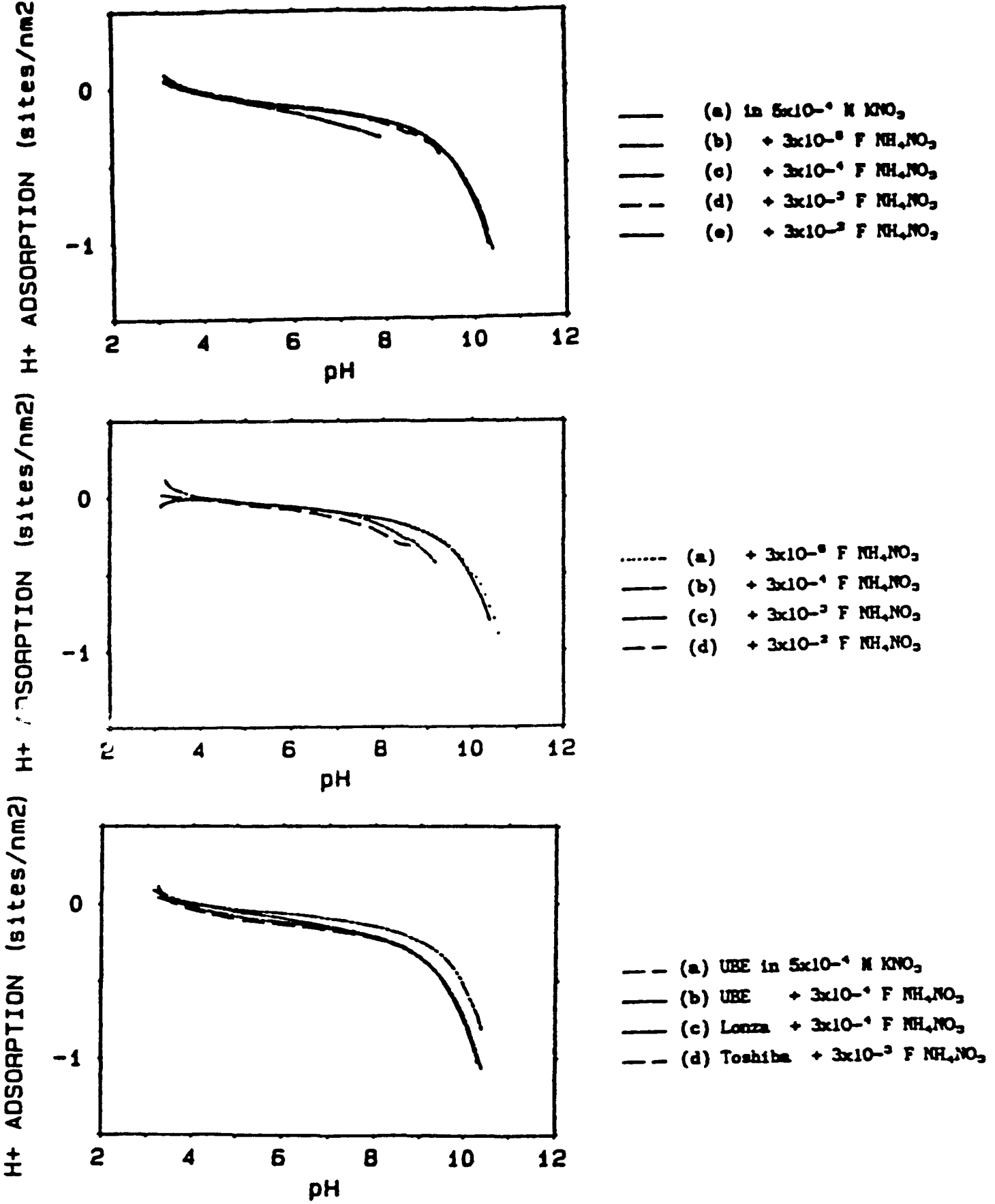

Figure 12

Effect of NH_3NO_4 addition on the relative adsorption curves for materials titrated in 5×10^{-4} M KNO_3 : (A) Cabosil silica titrated in increasing NH_4NO_3 concentration; (B) UBE silicon nitride titrated in increasing NH_4NO_3 concentration; and (C) comparison of UBE and Toshiba silicon nitride and Lonza silicon carbide all titrated in 5×10^{-3} M KNO_3 + 3×10^{-4}F NH_4NO_3.

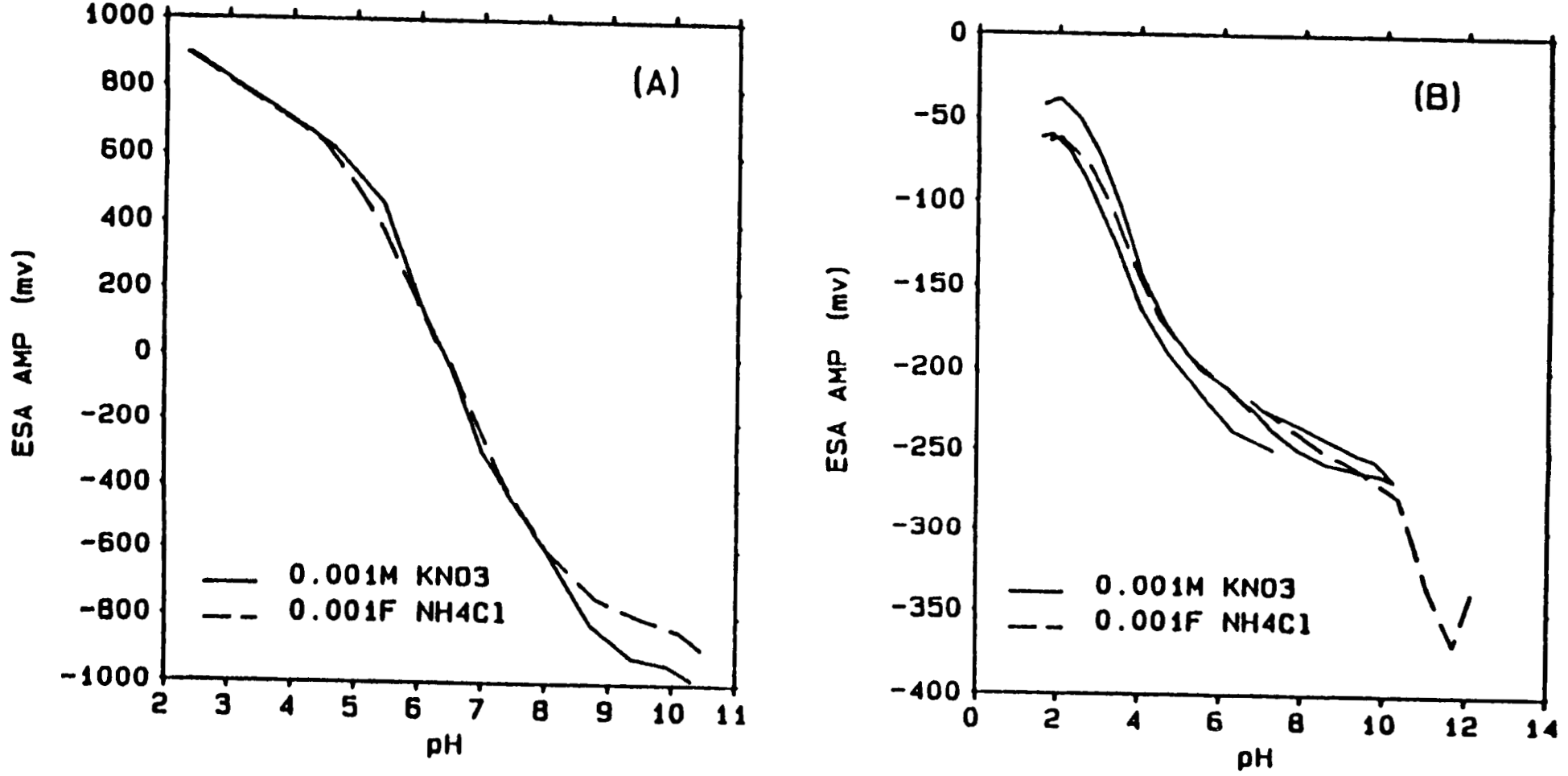

Figure 13

Variation in Electrokinetic Sonic Amplitude (ESA) vs. pH for silicon nitride powder in 0.001 F KNO_3 or NH_4NO_3 electrolyte: (A) 2 wt% sols of UBE silicon nitride, and (B) 2 wt% sols of Toshiba silicon nitride. Notice that the electrolyte species has no apparent effect on the ESA curves. Also note that the UBE silicon nitride crosses zero ESA amplitude (PZC) at pH 6.4 while the Toshiba powder exhibits no zero point.

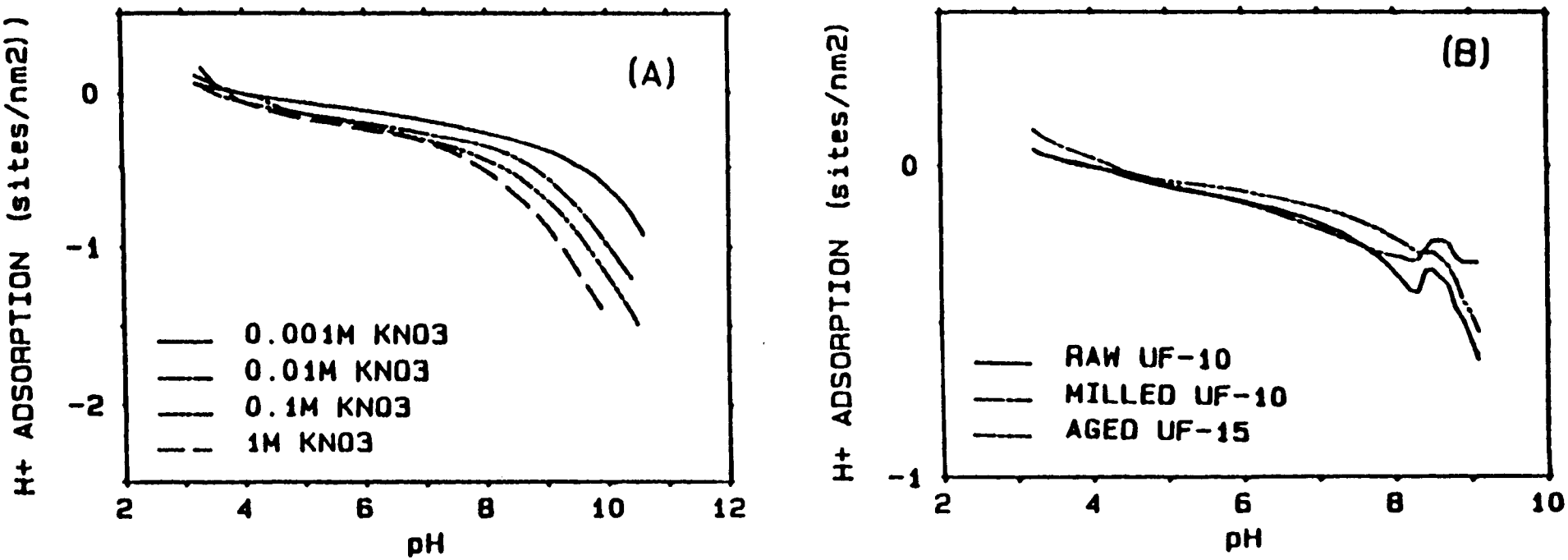

Figure 14

Effect of milling or aging Lonza silicon carbide powders in pH 9 NH_4NO_3 solution on titration results: (A) titration of milled Lonza UF-10 in increasing ionic strengths of KNO_3; (B) comparison of raw and milled Lonza UF-10 powder to UF-15 powder which was aged for 2 weeks in pH 9 NH_4NO_3. All of the curves in (B) were titrated in 5×10^{-4} M KNO_3 + 3×10^{-2}F NH_4NO_3.

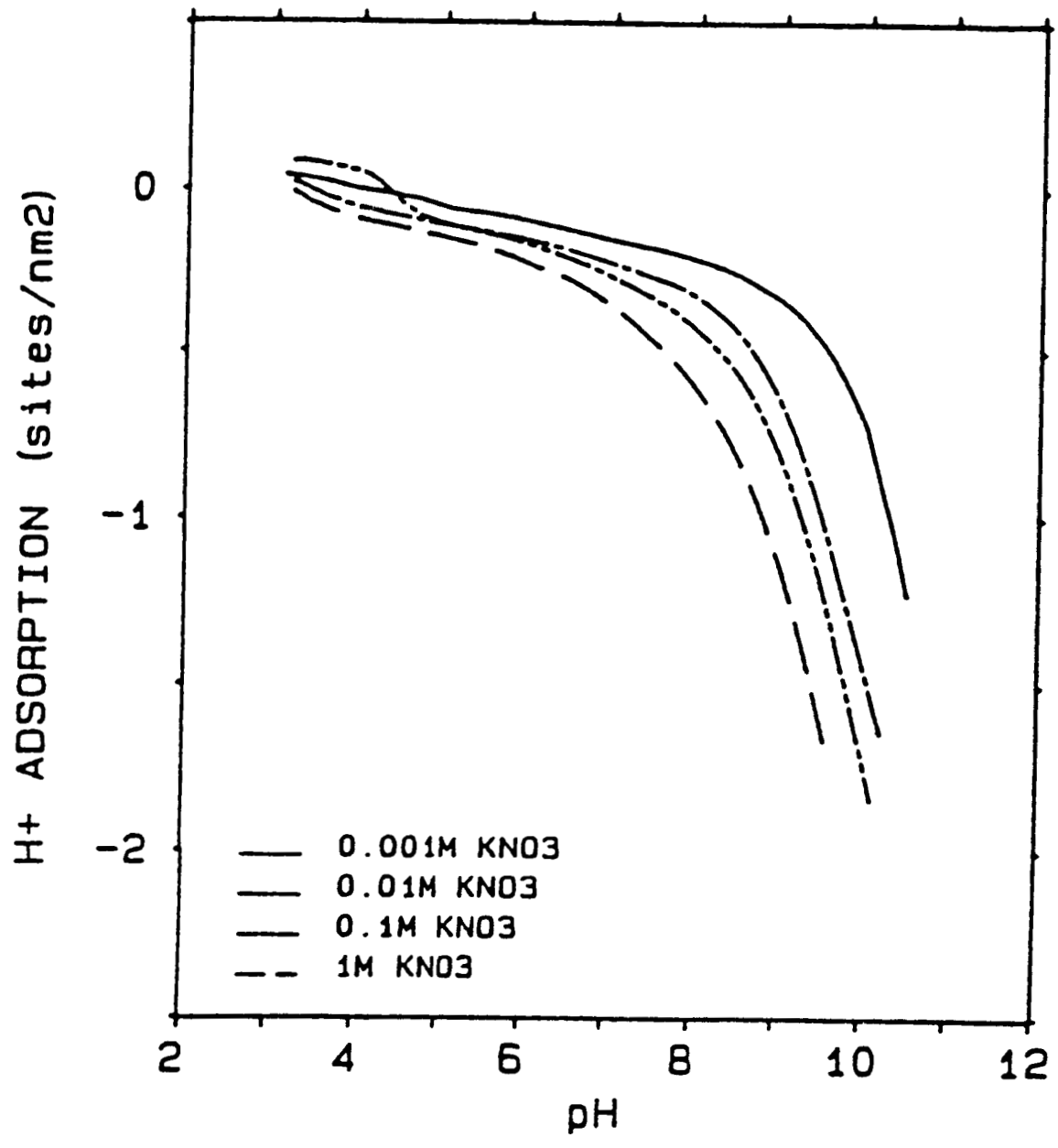

Figure 15

Relative adsorption titration curves for pretreated Toshiba silicon nitride powder in KNO_3 solutions of increasing ionic strength. Titration began at pH 3 in 0.001 M electrolyte and concluded back at pH 3 in 1M solution. Note that no obvious cip occurs in the pH region explored.

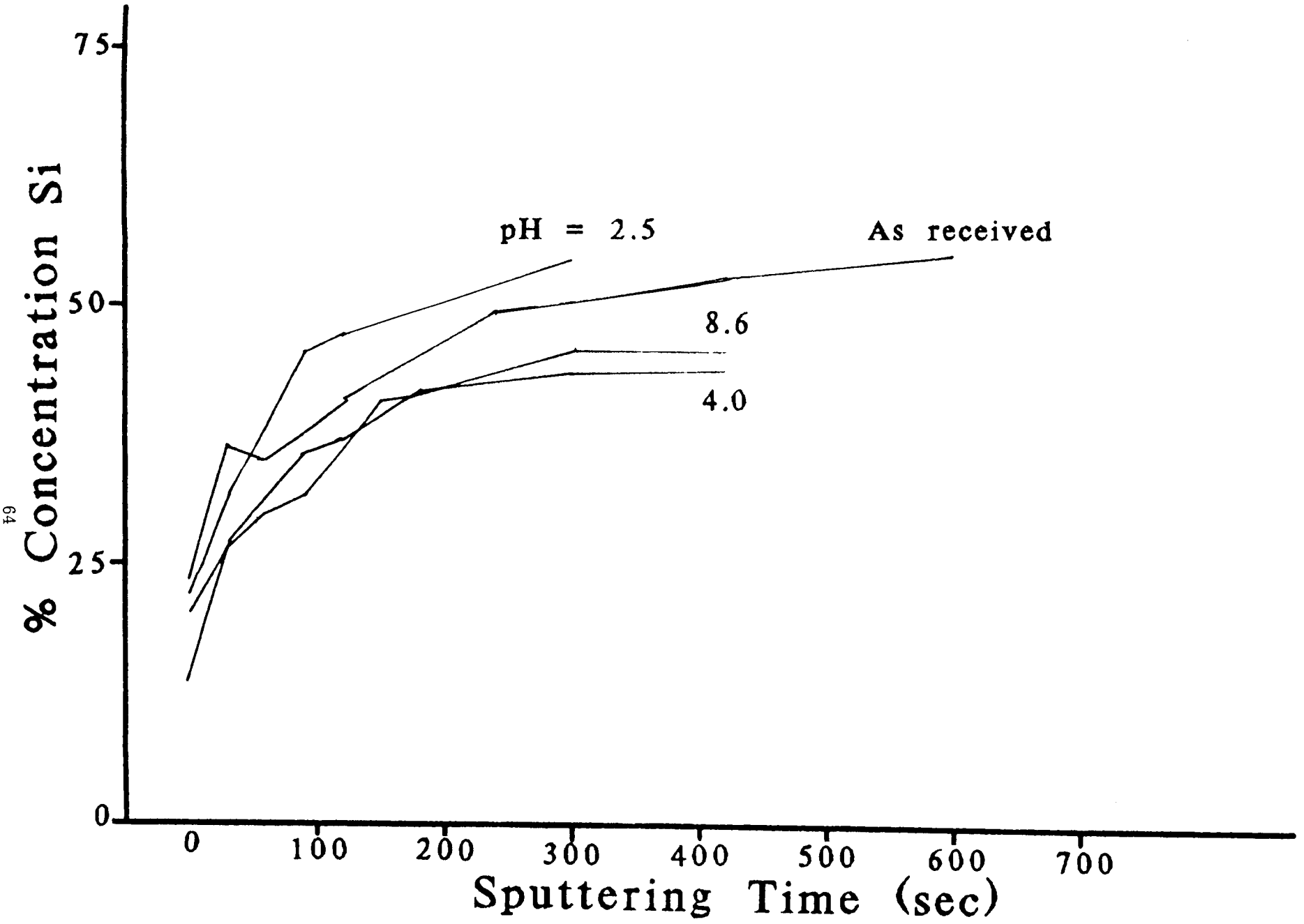

Figure 16
Effect of colloidal pretreatment on the interfacial chemistry of Lonza silicon carbide powder. Shown is the surface concentration of Si, as measured by AES, as a function of sputtering time (nominal sputtering rate 0.5 Å/sec) and pH of the washing pretreatment.

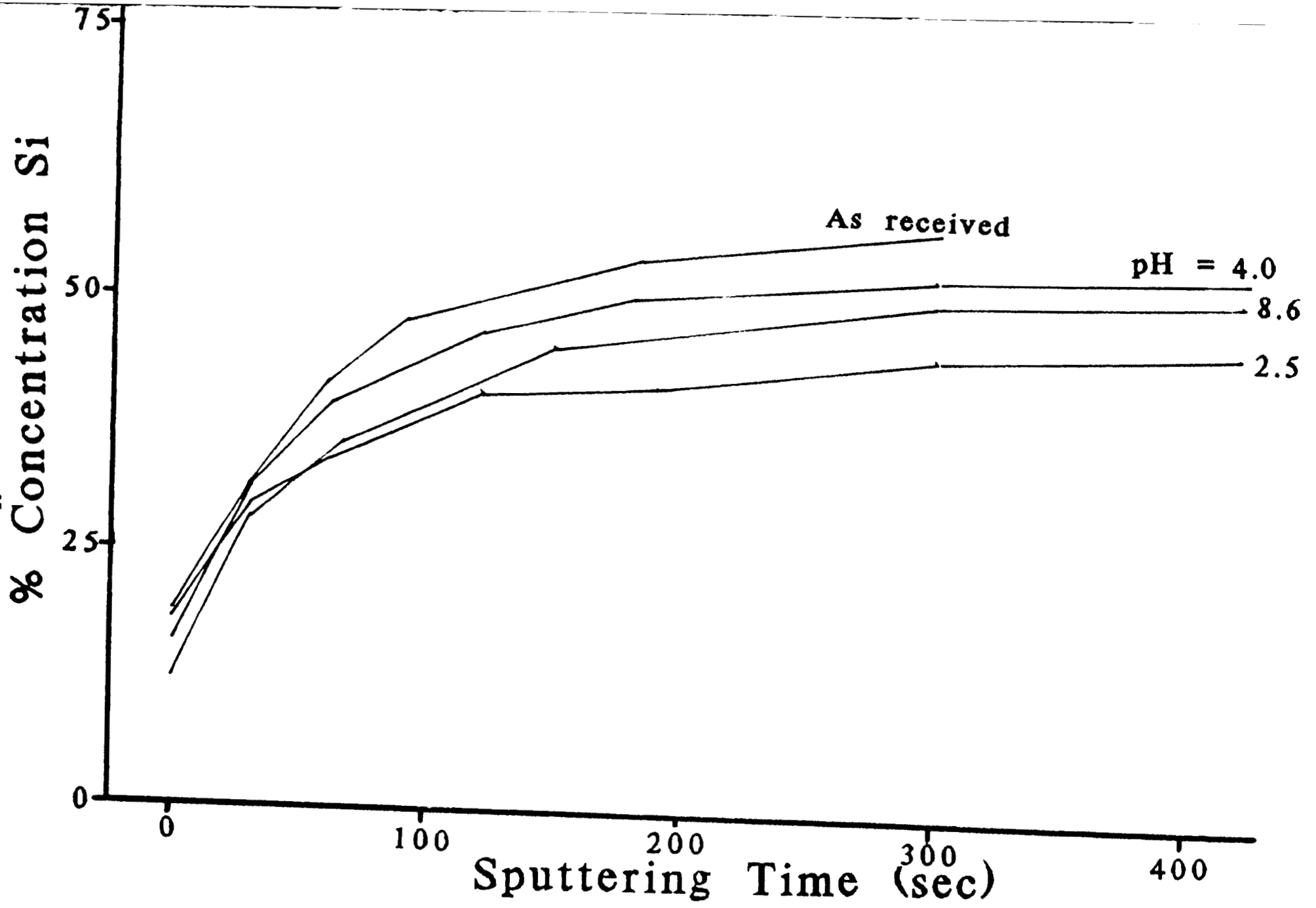

Figure 17
Effect of colloidal pretreatment on the interfacial chemistry of Arco silicon carbide fibers (same parameters as for Figure 16). Note the lasting effect of the colloidal pretreatment manifested in these results.

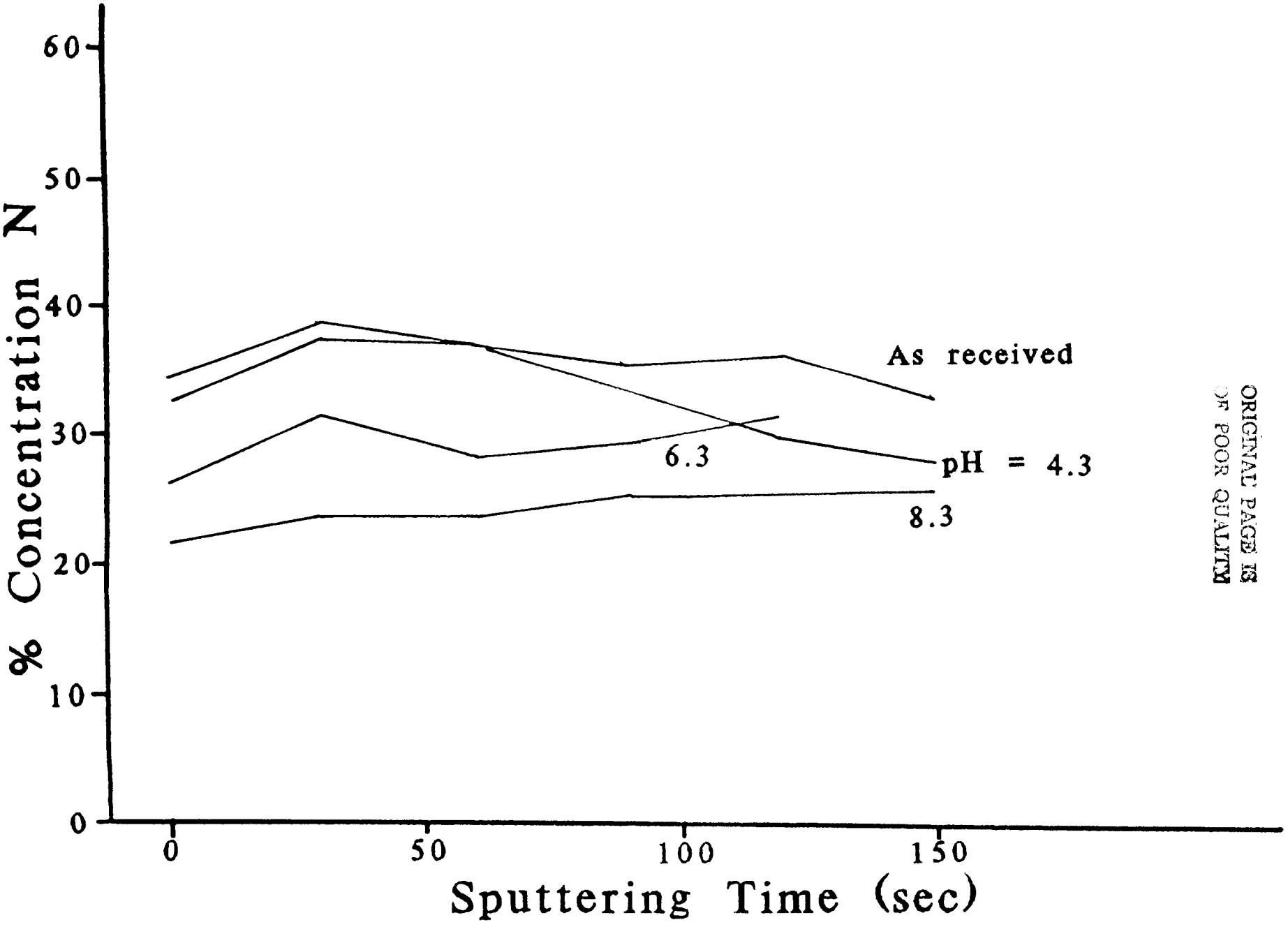

Figure 18
Effect of the colloidal pretreatment on the interfacial chemistry of UBE silicon nitride powder. Shown here is the surface concentration of N, as a function of sputtering time (nominal sputtering rate 1.0 Å/sec). Note that in this case as well, the interfacial composition has been affected by the

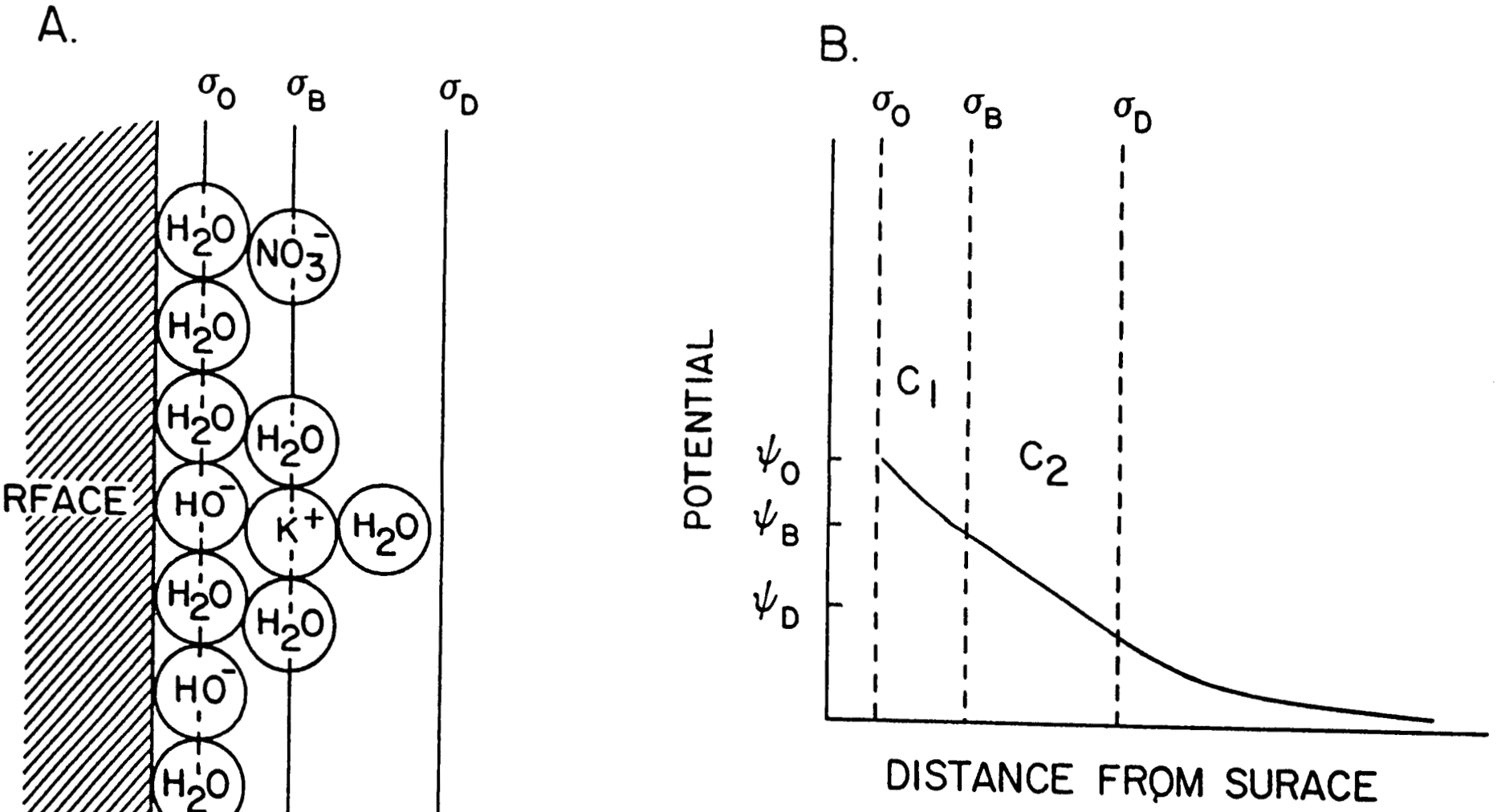

Figure 19
Schematic representation of the oxide-aqueous electrolyte interface as defined by Davis[28]: (A) location of the charged species comprising the various layers; (B) location of the equipotential planes.

Figure 20
Prediction of surface charge (A) and diffuse potential (B) for UBE silicon nitride using intrinsic ionization constants derived from the double extrapolation analysis. The predictions are compared to our titration measurement of surface charge and electrophoresis data.

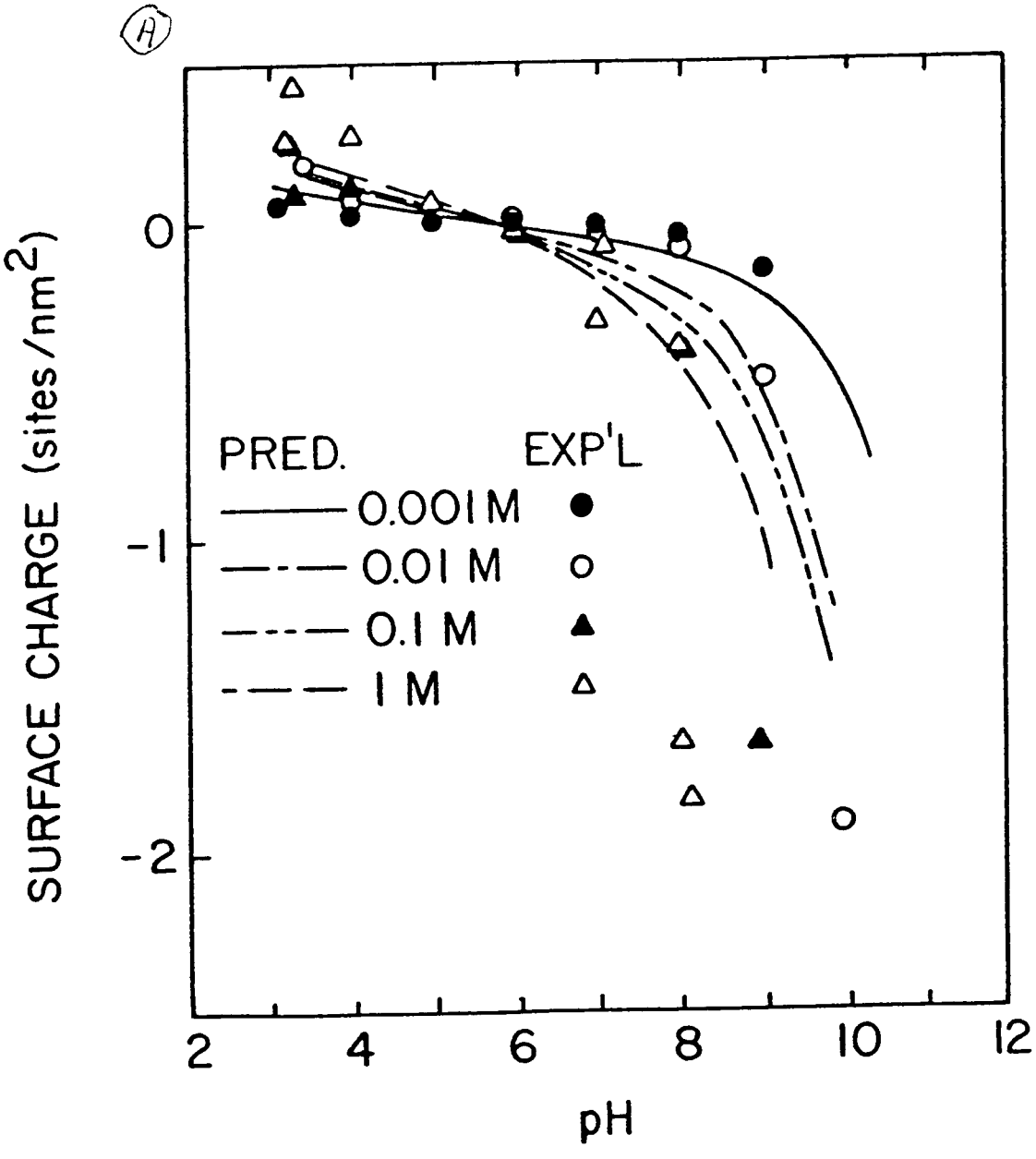

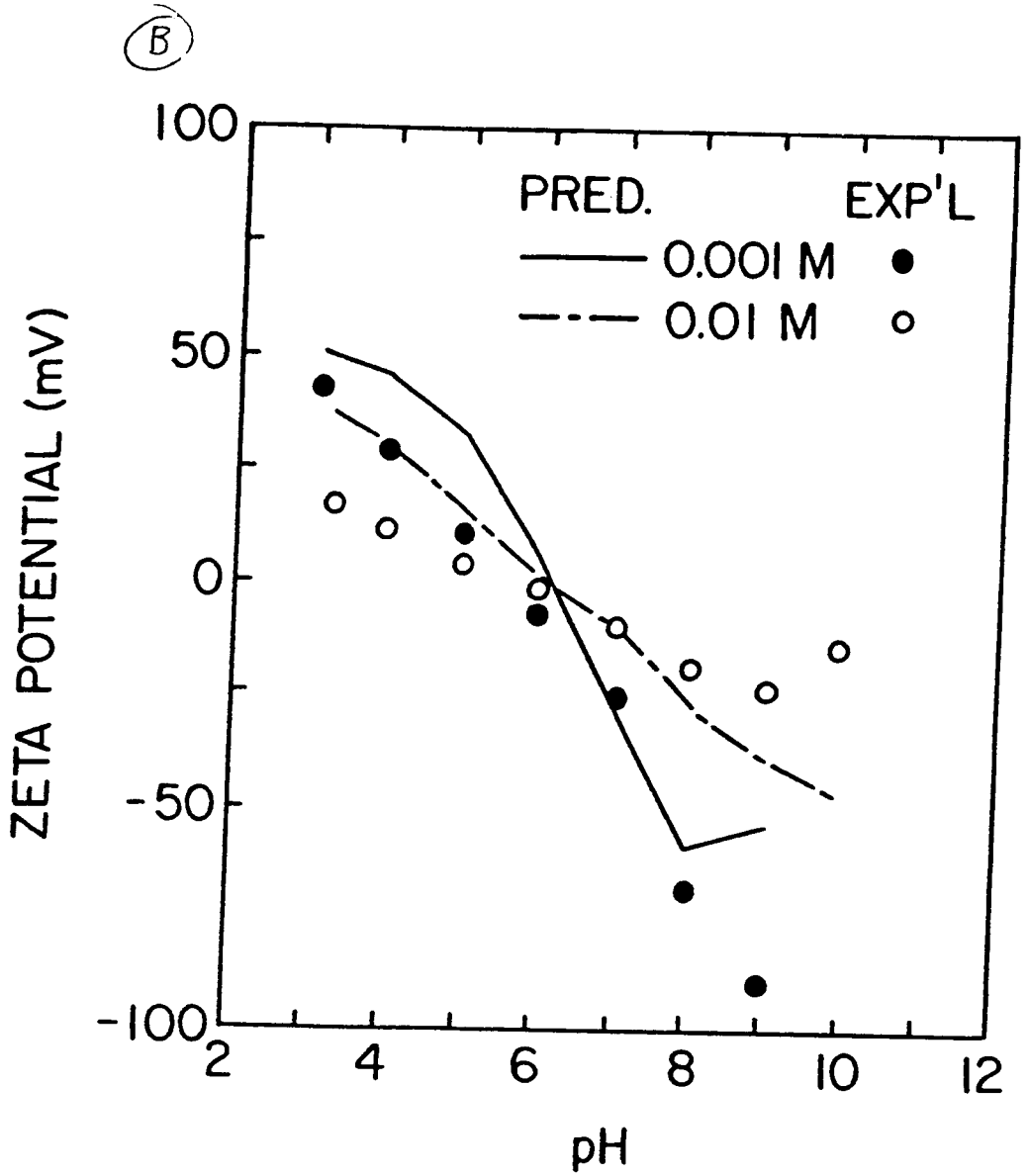
(B)
100
50
0
-50
-100
2
4
6
8
10
12
ZETA POTENTIAL (mV)
pH
PRED.
EXP'L
0.001 M
0.01 M

Figure 21
Prediction of surface charge for UBE silicon nitride using intrinsic ionization constants predicted by the regression scheme (Table 2) The predictions are compared to our titration measurements for surface charge.

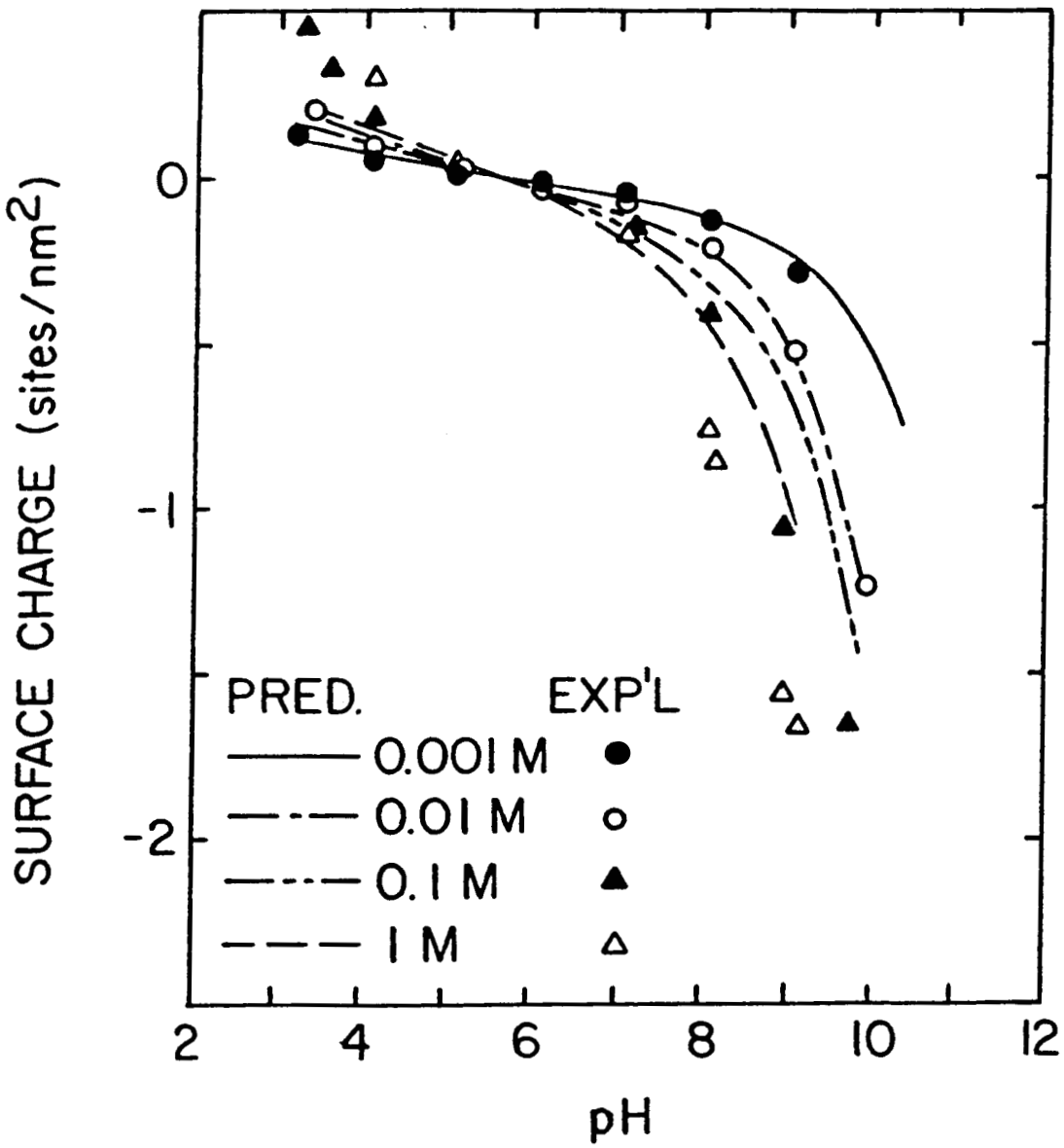

Figure 22

Prediction of diffuse layer potential for UBE silicon nitride using intrinsic ionization constants predicted by the regression scheme (Table 2). Zeta potential data is compared to the predicted diffuse layer potential (ψ_d).

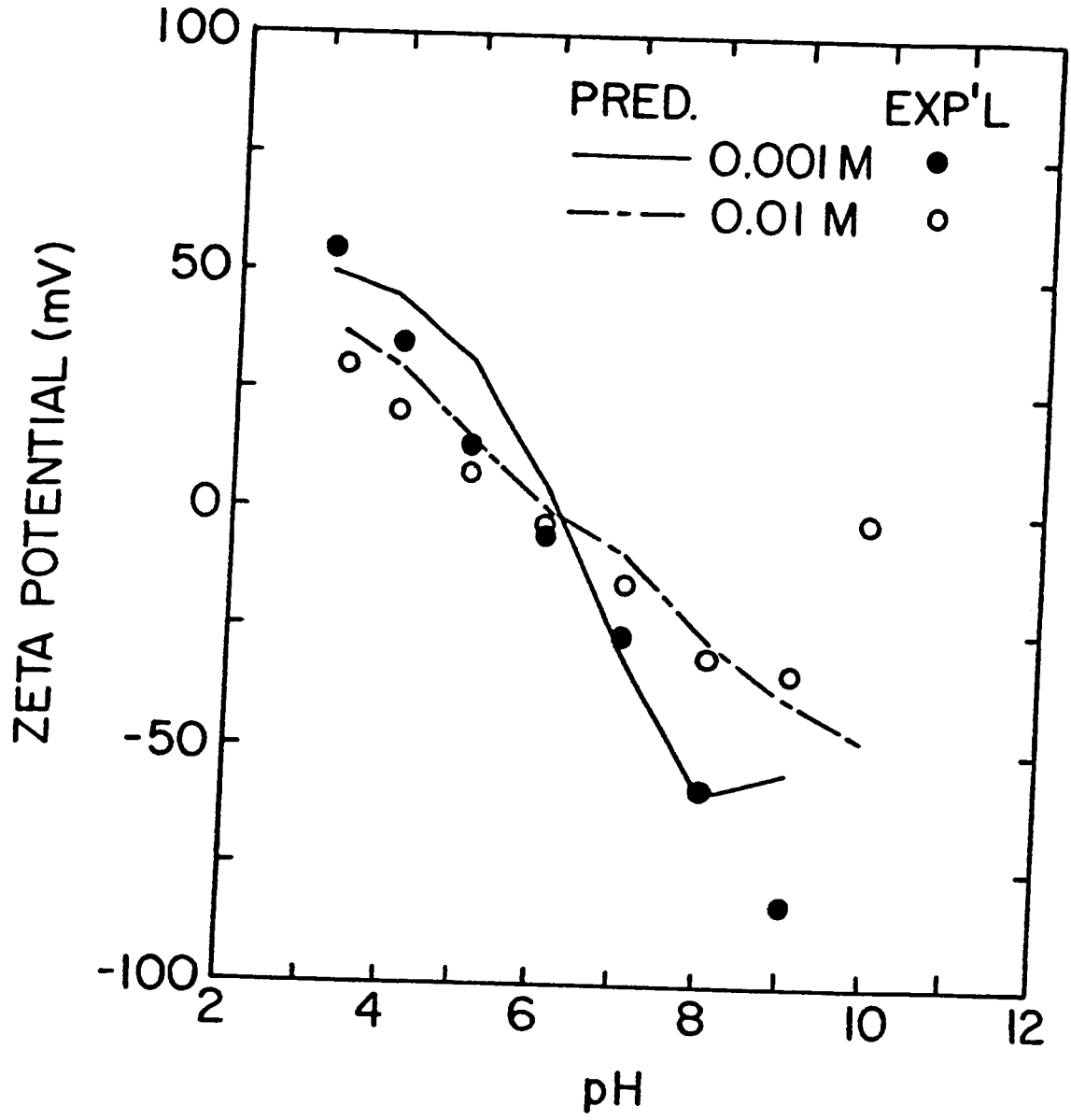

NASA
National Aeronautics and Space Administration

Report Documentation Page

1. Report No.	2. Government Accession No.	3. Recipient's Catalog No.
NASA CR-179634		

4. Title and Subtitle	5. Report Date
Stability and Rheology of Dispersions of Silicon Nitride and Silicon Carbide	June 1987
	6. Performing Organization Code

7. Author(s)	8. Performing Organization Report No.
Donald L. Feke	None
	10. Work Unit No. 533-05-11

9. Performing Organization Name and Address	11. Contract or Grant No.
Case Institute of Technology Case Western Reserve University Cleveland, Ohio 44106	NAG3-468
	13. Type of Report and Period Covered Contractor Report Final
12. Sponsoring Agency Name and Address	14. Sponsoring Agency Code
National Aeronautics and Space Administration Lewis Research Center Cleveland, Ohio 44135	

15. Supplementary Notes

Project Managers, Marc R. Freedman and Thomas P. Herbell, Materials Division, NASA Lewis Research Center.

16. Abstract

The relationship between the surface and colloid chemistry of commercial ultra-fine silicon carbide and silicon nitride powders has been examined by a variety of standard characterization techniques and by methodologies especially developed for ceramic dispersions. These include: surface titration; electrokinetic measurement; and surface spectroscopies. The effects of powder pretreatment and modification strategies, which can be utilized to augment control of processing characteristics, were monitored with these techniques. Both silicon carbide and nitride were found to exhibit silica-like surface chemistries, but silicon nitride powders possess an additional amine surface functionality. Colloidal characteristics of the various silicon nitride powders in aqueous suspension is believed to be highly dependent on the relative amounts of the two types of surface groups, which in turn is determined by the powder synthesis route. The differences in the apparent colloidal characteristics for silicon nitride powders cannot be attributed to the specific adsorption of ammonium ions. Development of a model for the prediction of double-layer characteristics of materials with a hybrid site interface facilitated understanding and prediction of the behavior of both surface charge and surface potential for these materials. The utility of the model in application to silicon nitride powders was demonstrated.

17. Key Words (Suggested by Author(s))	18. Distribution Statement
Ceramics; Silicon nitride; Silicon carbide; Rheology	Unclassified - unlimited STAR Category 27

19. Security Classif. (of this report)	20. Security Classif. (of this page)	21. No. of pages	22. Price*
Unclassified	Unclassified	73	A04

NASA FORM 1626 OCT 86

*For sale by the National Technical Information Service, Springfield, Virginia 22161